

What lies in between: Levallois, discoid and intermediate methods

Guillermo Bustos-Pérez

Guillermo Bustos-Pérez ^{1,2,3}, Javier Baena ¹, Manuel Vaquero ^{2,3}

¹ Universidad Autónoma de Madrid. Departamento de Prehistoria y Arqueología, Campus de Cantoblanco, 28049 Madrid, Spain

² Institut Català de Paleoecología Humana i Evolució Social (IPHES), Zona Educacional 4, Campus Sesclades URV (Edifici W3), 43007 Tarragona, Spain

³ Universitat Rovira i Virgili, Departament d’Història i Història de l’Art, Avinguda de Catalunya 35, 43002 Tarragona, Spain

Abstract

Lithic artefacts are usually associated with the different knapping methods used in their production. Flakes exhibit metric and technological features representative of the flaking method used to detach them. However, lithic production is a dynamic process in which discrete methods can be blurred, and in which features can vary throughout the process. An intermediate knapping method between the discoid and Levallois is commonly referred to under an umbrella of terms (the present research uses the term hierarchical discoid), and is associated with a broad geographical and chronological distribution throughout the Early and Middle Palaeolithic. This intermediate knapping strategy exhibits features of both the discoid and Levallois knapping methods, raising the question of the extent to which flakes from the three knapping methods can be differentiated and, when one is mistaken for another, the direction of confusion. An experimental assemblage of flakes detached by means of the three methods was used along with an attribute analysis and machine learning models in an effort to identify the knapping methods employed. In general, our results were able to very effectively differentiate between the three knapping methods when a support vector machine with polynomial kernel was used. Our results also underscored the singularity of flakes detached by means of Levallois reduction sequences, which yielded outstanding identification values, and were rarely erroneously attributed to either of the other two knapping methods studied. Mistaking the products of the discoid and hierarchical discoid methods was the most common direction of confusion, although a good identification value was achieved for discoid flakes and an acceptable value for hierarchical discoid flakes. This shows the potential applicability of machine learning models in combination with attribute analysis for the identification of these knapping methods among flakes.

Keywords: lithic technology; experimental archaeology; Levallois; discoid; Middle Palaeolithic; machine learning

Extended abstract

La producción de lascas se asocia a diferentes métodos de talla. Las lascas resultantes presentan características métricas y atributos que son representativos del método de talla del que se han producido. Sin embargo, la talla lítica es un proceso dinámico en el que los métodos de talla definidos pueden verse entremezclados debido a adaptaciones a las características volumétricas y de calidad de la materia prima, diferentes fases a lo largo del proceso de reducción, aspectos cronoculturales, etc. Esto da lugar a que las características de los productos de talla varíen a lo largo del proceso de reducción. Bajo diferentes términos es común encontrar alusiones a un método de talla intermedio entre el discoide y el Levallois, presentando una amplia distribución geográfica y cronológica a lo largo del Paleolítico Medio y el Paleolítico Medio inicial. La concepción de este método de talla, referido en el presente documento como Discoide Jerárquico, posee características intermedias entre el Levallois (jerarquización de superficies no intercambiables o un plano de talla paralelo a la intersección de ambas superficies) y el discoide (ausencia de preparación de talones, planos de talla secantes en la fase inicial de talla), surgiendo la duda de hasta qué se pueden diferenciar los productos de

lascado de los tres métodos y sobre la direccionalidad de las confusiones.

El presente trabajo emplea un conjunto experimental de lascas procedentes de los tres métodos de talla (77 del método de talla discoide, 73 del Levallois y 72 del Discoide Jerárquico). Sobre este conjunto experimental de lascas se realiza un análisis métrico y de atributos, y sobre los datos procedentes de este análisis se entrena diez algoritmos de aprendizaje automático con el objetivo de determinar hasta qué punto es posible diferenciar el método de talla. Para evaluar los algoritmos de aprendizaje automático se tiene en cuenta la precisión general de los modelos, pero también los efectos del uso de umbrales de probabilidad en la identificación de los métodos de talla. El uso de umbrales de probabilidad permite optimizar el ratio de positivos verdaderos y positivos falsos para cada umbral de decisión y de ahí extraer el “área bajo la curva” (AUC en inglés) como valor de evaluación de un modelo.

De los diez algoritmos de aprendizaje automático, una máquina de vector soporte con kernel polinomial presenta los mejores resultados en la identificación de los tres métodos de talla, proporcionando unos resultados excelentes a la hora de diferenciar entre los tres métodos a nivel general (0.667 precisión, 0.824 AUC). Considerando individualmente cada método de talla, los resultados subrayan el carácter singular de las lascas procedentes de secuencias de reducción Levallois ya que obtienen una identificación excepcionalmente buena (AUC de 0.91), siendo su procedencia raramente atribuida a cualquiera de los otros dos métodos. La confusión entre productos procedentes de secuencias de talla discoide y el Discoide Jerárquico es más común, aunque se alcanza una identificación excelente en el caso de los productos procedentes de reducciones discoides (AUC de 0.82) y una identificación aceptable en el caso los productos procedentes del Discoide Jerárquico (AUC de 0.73).

Estos resultados muestran el potencial de combinar modelos de aprendizaje automático con análisis de atributos sobre lascas para la identificación de métodos de talla. Su uso puede servir de gran ayuda en la identificación de métodos de talla en lascas. Sin embargo, su uso requiere de una evaluación previa de los conjuntos líticos para determinar posibles métodos de talla existentes, uso diferencial de las materias primas, y evaluación de las cadenas operativas presentes.

Palabras clave: tecnología lítica; arqueología experimental; Levallois; Discoid; Paleolítico Medio; Aprendizaje Automático

1. Introduction

The Middle Palaeolithic in western Europe is characterised by the increase in and diversification of prepared core knapping methods, resulting in flake-dominated assemblages ([Kuhn 2013](#)). These flake-dominated assemblages are the result of a wide number of production methods including Levallois ([Boëda 1994](#); [Boëda 1995b](#); [Boëda et al. 1990](#)), discoid ([Boëda 1993](#); [Boëda 1995a](#)), the *système par surface de débitage alterné* or SSDA ([Forestier 1993](#); [Ohel et al. 1979](#)), Quina ([Bourguignon 1996](#); [Bourguignon 1997](#)), different laminar production systems ([Boëda 1990](#); [Révillon & Tuffreau 1994](#)), and the Kombewa ([Newcomer & Hivernel-Guerre 1974](#); [Tixier & Turq 1999](#)) among several others. This abundance of different production methods results in a highly diversified material culture in which flakes exhibit great morphological variability. Flakes often retain morphologies and attributes characteristic of the knapping method used to detach them, facilitating the identification of those methods. However, flakes also often present overlapping attributes and morphologies as a result of the high internal variability of the methods used and the fact that flakes with similar functional properties can be produced via different methods [Kuhn \(2013\)](#). Due to their extensive geographical and chronological distribution, the Levallois and discoid constitute important sources of cultural variability in the Middle Palaeolithic of western Europe.

[Boëda \(1994; 1995b\)](#) establishes six characteristics that define the Levallois knapping strategy from a technological perspective:

- 1) The volume of the core is conceived in two convex asymmetric surfaces.

- 2) These two surfaces are hierarchical and are not interchangeable. They retain their role of either striking or debitage (or exploitation) surface throughout the entire reduction process.
- 3) The distal and lateral convexities of the debitage surface are maintained to obtain predetermined flakes.
- 4) The plane of fracture of the predetermined products is parallel to the intersection of the two surfaces.
- 5) The striking platform is perpendicular to the overhang (the core edge, at the intersection between the two core surfaces).
- 6) The technique employed during the knapping process is direct percussion with a hard hammer.

Depending on the organisation of the debitage surface, Levallois cores are usually classified as a preferential method (in which a single predetermined Levallois flake is obtained from the debitage surface) or as recurrent methods (in which several predetermined flakes are produced from the debitage surface) with removals being either unidirectional, bidirectional or centripetal (Boëda 1995b; Boëda *et al.* 1990; Delagnes 1995; Delagnes & Meignen 2006).

Because of its early recognition in the XIX century (Mortillet 1885: pp.:235–236), its association with the cognitive abilities of planning and predetermination (Boëda 1994; Pelegrin 2009), and its use for the definition of cultural facies (Bordes 1961a; Bordes 1953) and lithic technocomplexes (Delagnes *et al.* 2007; Faivre *et al.* 2017), Levallois flaking technology is considered a trademark of the Middle Palaeolithic. The emergence of the Levallois method has been observed from MIS 12 to MIS 9, with several sites yielding artefacts characteristic of this knapping strategy (Carmignani *et al.* 2017; Hérisson *et al.* 2016; Moncel *et al.* 2020; Soriano & Villa 2017; White & Ashton 2003). However, the Levallois is clearly generalised and identified from MIS 8 onwards, covering an extensive geographical area throughout western Europe (Delagnes *et al.* 2007; Delagnes & Meignen 2006; Faivre *et al.* 2017; Geneste 1990). The extensive geographical area and long temporal span of the Levallois creates additional layers of variability which can result from raw material constraints, synchronic variability as a result of different site functionalities, chronological trends in the development of methods, or shifts in the technological organisation of groups. It is also important to highlight the explicit recognition of Levallois cores after MIS 8, while a multitude of terms were employed to define previous hierarchical knapping strategies and their possible coexistence with Acheulean technocomplexes (Moncel *et al.* 2020; Santonja *et al.* 2016; Hérisson *et al.* 2016; Rosenberg-Yefet *et al.* 2022; White & Ashton 2003; Scott & Ashton 2011).

Boëda (1993; 1994; 1995a), also establishes six technological criteria defining the discoid method:

- 1) The volume of the core is conceived as two oblique asymmetric convex surfaces delimited by an intersection plane.
- 2) These two surfaces are not hierarchical as it is possible to alternate the roles of the percussion and exploitation surfaces.
- 3) The peripheral convexity of the debitage surface is managed to control lateral and distal extractions, thus allowing for a certain degree of predetermination.
- 4) Striking surfaces are oriented so that the core edge is perpendicular to the predetermined products.
- 5) The planes of extraction of the products are secant.
- 6) The technique employed is direct percussion with a hard hammer.

Technological analyses of Middle Palaeolithic assemblages have gradually led to the identification of a variability of modalities within discoid core knapping (Bourguignon & Turq 2003; Locht 2003; Terradas 2003;

Locht 2003). This has resulted in *sensu stricto* and a *sensu lato* conceptualisations of the discoid knapping system (Fairev *et al.* 2017; Mourre 2003; Thiébaut 2013). The *sensu stricto* method closely corresponds to the definition established by Boëda (1993) described above, for which core edge flakes and pseudo-Levallois points are the most common products. The *sensu lato* discoid encompasses a greater range of products (although centripetal flakes are more common) as a result of higher variability in the organisation of percussion and exploitation surfaces (Terradas 2003).

One of the variants of the *sensu lato* discoid conceptualisation resembles the Levallois knapping strategy (Figure 1). Several common characteristics have been defined for this method:

- 1) The core volume is conceived as two hierarchical asymmetric surfaces: the percussion surface and the exploitation surface (this feature is shared with the Levallois).
- 2) Preparation of the percussion surface is absent or partial, without encompassing the complete periphery of the core. This may be because the characteristics of the raw material present an adequate morphology or because it requires minimal preparation.
- 3) Despite the hierarchical nature of the two surfaces, flakes detached from the debitage surface present a secant relationship towards the plane of intersection. Soriano and Villa (2017) point out that Levallois products usually present an external platform angle (EPA) of between 80° and 85° , while products from non-Levallois hierarchical methods present an EPA relationship of between 70° and 85° . However, this relationship can change over the course of the core's reduction with the final flakes being sub-parallel to the plane of fracture (Slimak 1998).
- 4) Products from the hierarchical discoid method tend to be symmetrical towards the knapping direction and thin, and the ventral and dorsal surfaces present a subparallel relationship. Again, these are common traits in Levallois products as well.

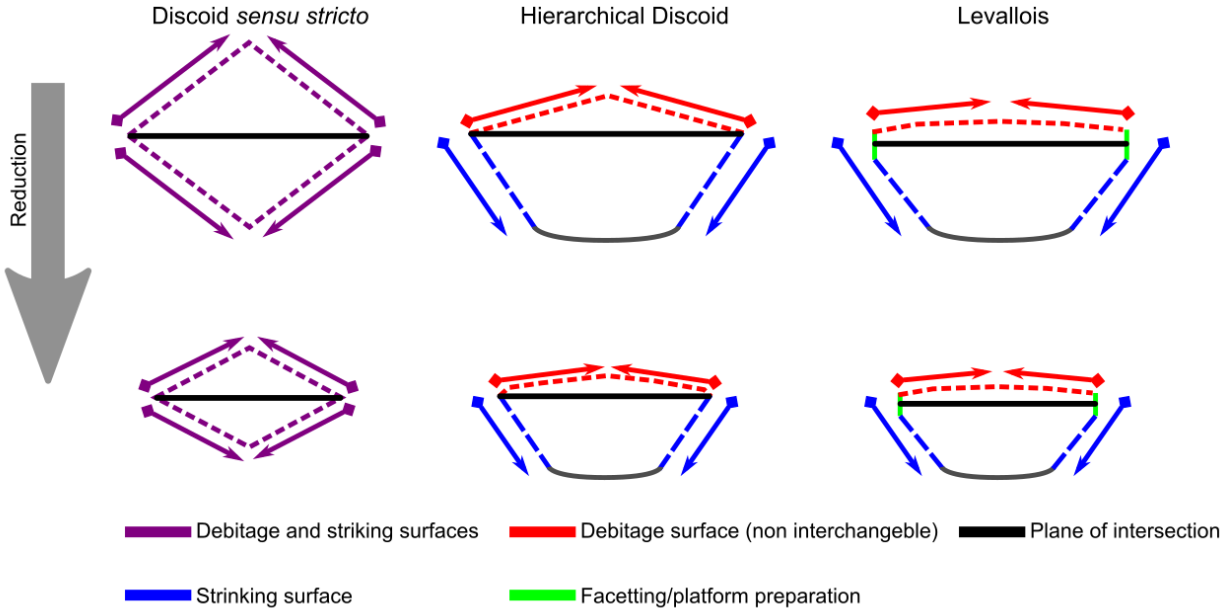


Figure 1: Schematic representation of the knapping methods, surfaces and platform preparation

Strategies evidenced at several sites fit into the discoid knapping variation described above, and its resemblance to the Levallois has been previously noted in several Middle and early Middle Palaeolithic assemblages (Casanova i Martí *et al.* 2009; 2014; Jaubert 1993; Peresani 1998; Slimak 1998; 2003; Soriano & Villa 2017).

However, it is important to consider that a variety of different terms have been employed due to the broad geographical and chronological span of the method. For Middle Palaeolithic sites, the identification of this method usually focuses on its shared features with the Levallois and discoid methods and thus, its intermediate nature.

Jaubert (1993), at Mauran, noted the hierarchical nature of the production system and its resemblance to exhausted recurrent centripetal Levallois cores. However, he pointed out that the secant planes of detachment were not as parallel as in the Levallois. Slimak (1998; 2003), at Champ Grand, also noted the similarities of residual cores with recurrent centripetal Levallois debitage. At Estret de Tragó, Casanova i Martí et al. (2009; 2014) noted the presence of products and knapping methods which shared features of the Levallois and discoid methods, and proposed including the hierarchical discoid and Levallois recurrent centripetal strategies within a single hierarchical bifacial centripetal class. Peresani (1998) at Fumane cave, documented the presence of debitage products with features (reduced thickness, debitage angle, and centripetal organisation of scars also subparallel to the ventral surface) which would correspond to parallel-plane debitage. Baena et al., (2005) indicated the presence of the hierarchical discoid method throughout the Esquilleu cave sequence as a secondary and primary knapping method.



Figure 2: Distribution of sites referenced in the text base map obtained from: <https://maps-for-free.com/>)

As mentioned earlier, for Middle Palaeolithic sites, the identity of this knapping method is focused on its intermediate nature, as something between the discoid method and the recurrent centripetal Levallois.

However, at early Middle Palaeolithic sites, the identification of this method usually focuses on its shared features with the Levallois, as a method that preceded the gradual emergence of the Levallois. For example, Carmignani *et al.* (2017) used the term “centripetal with parallel planes”, noting the resemblance of some features to those of the Levallois at the sites of Payre and Bau de l’Aubesier. Soriano & Villa (2017) at Guado San Nicola, used the term “non-Levallois debitage with hierarchised surfaces”, noting its similarity to the Levallois, but also its distinctiveness, due to the absence of preparation and management of convexities and the lack of platform preparation. For Cuesta de la Bajada Santonja *et al.* (2016) differentiate between Levallois cores and cores of centripetal character with preferential surfaces (which are simply referred to as centripetal). Lombera-Hermida *et al.* (2020) record the presence of “predetermined hierarchical centripetal” cores in different raw materials in TD10.1 at Atapuerca, and note the differences to and coexistence with classical discoid and Levallois knapping methods. The use of terms alluding to the hierarchical and centripetal nature of this method is not limited to European sites; the term “hierarchical bifacial centripetal” was used to refer to the Oldowan industries of Peninj (Torre *et al.* 2003).

The technological criteria for identifying production systems are clearly visible on cores. However, a high degree of uncertainty remains when examining flakes, as the technological criteria are less evident or absent (Hovers 2009). Another underlying cause is the fluid and continuous nature of lithic knapping and reduction which can blur differences between apparently clear-cut methods. Additionally, variations can result from adaptations to raw materials (different knapping methods applied to different raw materials in the same archaeological level), the initial morphology of the raw material, the knappers expertise and stage in the learning process and/or circumstantial events and restrictions. This adds up to an absence of discrete categories that are blurred by the underlying existence of a wide variety of lithic expressions. The attribution of flakes to a knapping method tends to be based on observed features compared with experimental collections, the context given from the knapping methods observed in the cores of the assemblage (although cores in an assemblage do not necessarily represent all knapping methods), and, importantly, the experience of the analyst. (Hovers 2009; Perpère 1986; Bisson 2000) Perpère (1986; 1989) have illustrated that using a dual classification category of Levallois or non-Levallois results in 30% disagreement among researchers. However, it is important to note that Perpère’s work (1986; 1989) anticipates Boëda’s volumetric and technological criteria (Boëda (1994); Boëda (1995b); Boëda *et al.* (1990)) which have contributed to decreasing the degree of disagreement in the identification of the Levallois. Another example of classification discrepancy comes from the type counts conducted by Dibble and Tuffreau at the Biache Saint-Bass site, in which Levallois flakes represented 46.08% of the assemblage in one list and 27.29% in the other (Dibble 1995).

Thus, a strong argument can be made for the difficulty of attributing knapping methods to flakes. This difficulty increases due to the existence of intermediate methods such as the hierarchical discoid, whose technological characteristics fall between the *sensu stricto* discoid and the Levallois. This work uses products experimentally knapped using the Levallois, discoid, and hierarchical discoid methods and a machine learning approach to address this problem. Our results provide insight into the classification accuracy for each knapping method, variable importance, and the directions of confusion between methods.

1.2 Introduction: loading packages and data

The following lines of code load packages employed for the development of the present study. Packages employed are: tidyverse (Wickham *et al.* 2019), caret (Kuhn 2008) and pROC (Robin *et al.* 2011).

Please note that all data necessary for the development of the present study along with the original Machine Learning models is freely available at the corresponding repository. This script loads an *.RData* file which contains a tibble with clean data and established factors. Additionally a *.csv* file containing the same data is available.

The following line of code loads the above mentioned packages.

```
# Load libraries
library(tidyverse); library(caret); library(pROC)
```

The following lines of code load and shows the *.RData* file containing the data employed for the analysis.

```

# Load the data
load("Data/Data.RData")

# Print first ten rows and first ten columns
print(ML_Data[1:10, 1:10])

## # A tibble: 10 x 10
##   Artifact_ID Core     Class Knapp~1 Frag_~2 Compl~3 Length Width Lamin~4 MeanT~5
##   <chr>        <chr>    <fct>  <chr>   <chr>    <dbl> <dbl>  <dbl>  <dbl>
## 1 Disc_08_01 Discoid_08 D      Full P~ C       Y      40.4  31.4  1.29   4.67
## 2 Disc_08_02 Discoid_08 D      Full P~ C       Y      42.2  41.6  1.01   10.7
## 3 Disc_08_03 Discoid_08 D      Full P~ C       Y      28.9  38.5  0.751  9.17
## 4 Disc_08_04 Discoid_08 D      Full P~ C       Y      58.6  39.4  1.49   12.0
## 5 Disc_08_05 Discoid_08 D      Full P~ C       Y      41    35.1  1.17   11.3
## 6 Disc_08_06 Discoid_08 D      Full P~ C       Y      40.2  28    1.44   11.9
## 7 Disc_08_07 Discoid_08 D      Full P~ C       Y      36.8  30.7  1.20   8.4
## 8 Disc_08_08 Discoid_08 D      Full P~ C       Y      41.7  28.4  1.47   6.93
## 9 Disc_08_09 Discoid_08 D      Full P~ C       Y      46.7  27.8  1.68   6.67
## 10 Disc_08_10 Discoid_08 D     Full P~ C       Y      49.2  23.1  2.13   7.73
## # ... with abbreviated variable names 1: Knapping_Phase, 2: Frag_Cat, 3: Complete,
## #   4: Laminar_Index, 5: MeanThick

# Print first ten rows and last 5 columns
print(ML_Data[1:10, ncol(ML_Data)-5:ncol(ML_Data)])

```

```

## # A tibble: 10 x 32
##   Flake_Type Trans~1 Termi~2 Long_~3 No_Sc~4 Corte~5 Cortex Plat_~6 Plat_~7 Flake~8
##   <chr>        <chr>    <chr>    <dbl>  <dbl>  <dbl> <dbl> <chr>  <chr>    <dbl>
## 1 Backed Fl~ Trapez~ Feather    0     2     5     5 L    RT    165.
## 2 Flake       Triang~ Feather   0     3     5     5 L    CX    5.56
## 3 Flake       Trapez~ Feather   0     3     5     5 D    BF    5.28
## 4 Flake       Triang~ Feather   0     4     5     5 L    CX    69.8
## 5 Backed Fl~ Trapez~ Feather   0     3     5     5 L    RT    23.7
## 6 Backed Fl~ Triang~ Feather   0     3     5     5 L    RT    29.1
## 7 Backed Fl~ Triang~ Feather   0     2     5     5 L    RT    32.2
## 8 Flake       Triang~ Feather   2     2     2     4 L    CC    10.8
## 9 Backed Fl~ Triang~ Feather   0     2     5     5 L    CX    20.1
## 10 Flake      Triang~ Feather  0     3     5     5 L   RT    22.9
## # ... with 22 more variables: Plat_Width <dbl>, Plat_Depth <dbl>,
## #   Surface.Plat <dbl>, Curvature <dbl>, Weight <dbl>, CVThick <dbl>,
## #   SDThick <dbl>, Angle_Lat_Marg <dbl>, Surf_Thickness <dbl>, Surf_Area <dbl>,
## #   CarenIndex <dbl>, Max_Thickness <dbl>, MeanThickness <dbl>, Laminar_Index <dbl>,
## #   Width <dbl>, Length <dbl>, Complete <chr>, Frag_Cat <chr>,
## #   Knapping_Phase <chr>, Class <fct>, Core <chr>, Artifact_ID <chr>, and
## #   abbreviated variable names 1: Trans_Section, 2: Termination_type, ...

```

2. Methods

An attribute analysis was performed on an experimental assemblage of flakes detached by means of the Levallois, discoid and hierarchical discoid reduction sequences. Supervised machine learning models were trained on the resulting dataset to identify the knapping method by which each flake was detached.

2.1 Experimental assemblage

The experimental assemblage consists of 222 experimentally knapped products resulting from Levallois, discoid and hierarchical discoid reduction sequences. It was knapped by two of the authors (JB and GBP), one of whom (JB) is considered a high-level expert, while the second (GBP) is considered an intermediate-high knapper. The Levallois (Boëda 1993; 1994; 1995b; Boëda *et al.* 1990) products belonged to the preferential and recurrent centripetal modalities. The hierarchical discoid cores were knapped in accordance with previous technological descriptions, with no platform preparation, with centripetal scar direction (although some opportunistic preferential flakes were obtained), and without deliberate management of convexities. The discoid. The discoid (Boëda 1993; Thiébaut 2013; Terradas 2003) products belonged to the *sensu stricto* conceptualisation in which both surfaces are bifacially knapped. With the Levallois and hierarchical discoid methods, only products from the debitage surface were included (flakes detached from the percussion surface were excluded from analysis). Because discoid knapping alternates the role of the percussion and debitage surfaces, all products were included. In all three cases, products from all stages of reduction were included (decortication, management of convexities, full production). To be sure of the surface to which each flake belonged and the completeness of each sequence, products were separated accordingly during the knapping sequence and, when that was not possible, cores and flakes were refitted. Only complete products were included, and all of the knapping sequences were carried out on different types of flint.

As previously noticed (Eren *et al.* 2008), the discoid system was the most productive, generating the highest number of flakes with the lowest number of cores. The flake counts for the Levallois and hierarchical discoid methods were similar per core and lower than those from the discoid cores. This was expected since only flakes from the production surface were included. It is important to note that this resulted in a very well-balanced dataset in which the sum of the products from each of the three classes was close to 33.33%. The distribution of the amount of cortex was similar across the knapping methods studied. In all cases, the sum of non-cortical flakes and flakes with residual cortex were similarly distributed among the three knapping strategies and made up the majority of flakes (near 60% in all three categories). A visual exploratory analysis of the assemblage using a scatter plot with Bagolini's categories (Bagolini 1968) showed that most of the flakes fall into the 'normal' and 'big' size categories, with hierarchical discoid flakes being slightly larger than flakes produced by means of discoid or Levallois reduction sequences. Additionally, most of the flakes from all three methods fall into the categories of 'elongated flakes', 'normal flakes' and 'wide flakes' in terms of their length to width ratios.

```
# Get number of cores and flakes (and their percentage) per class
ML_Data %>% group_by(Class) %>%
  summarise(
    Cores = n_distinct(Core),
    Flakes = n(),
    Percent = (Flakes/222)*100

## # A tibble: 3 x 4
##   Class Cores Flakes Percent
##   <fct> <int>   <int>   <dbl>
## 1 L         4       73     32.9
## 2 D         3       77     34.7
## 3 HD        7       72     32.4

# Cortex per class
ML_Data %>%
  group_by(Class, Cortex) %>%
  summarise(N = n()) %>%
  mutate(Percentage = (N/sum(N))*100) %>%

ggplot(aes(Class, Percentage, fill = factor(Cortex))) +
```

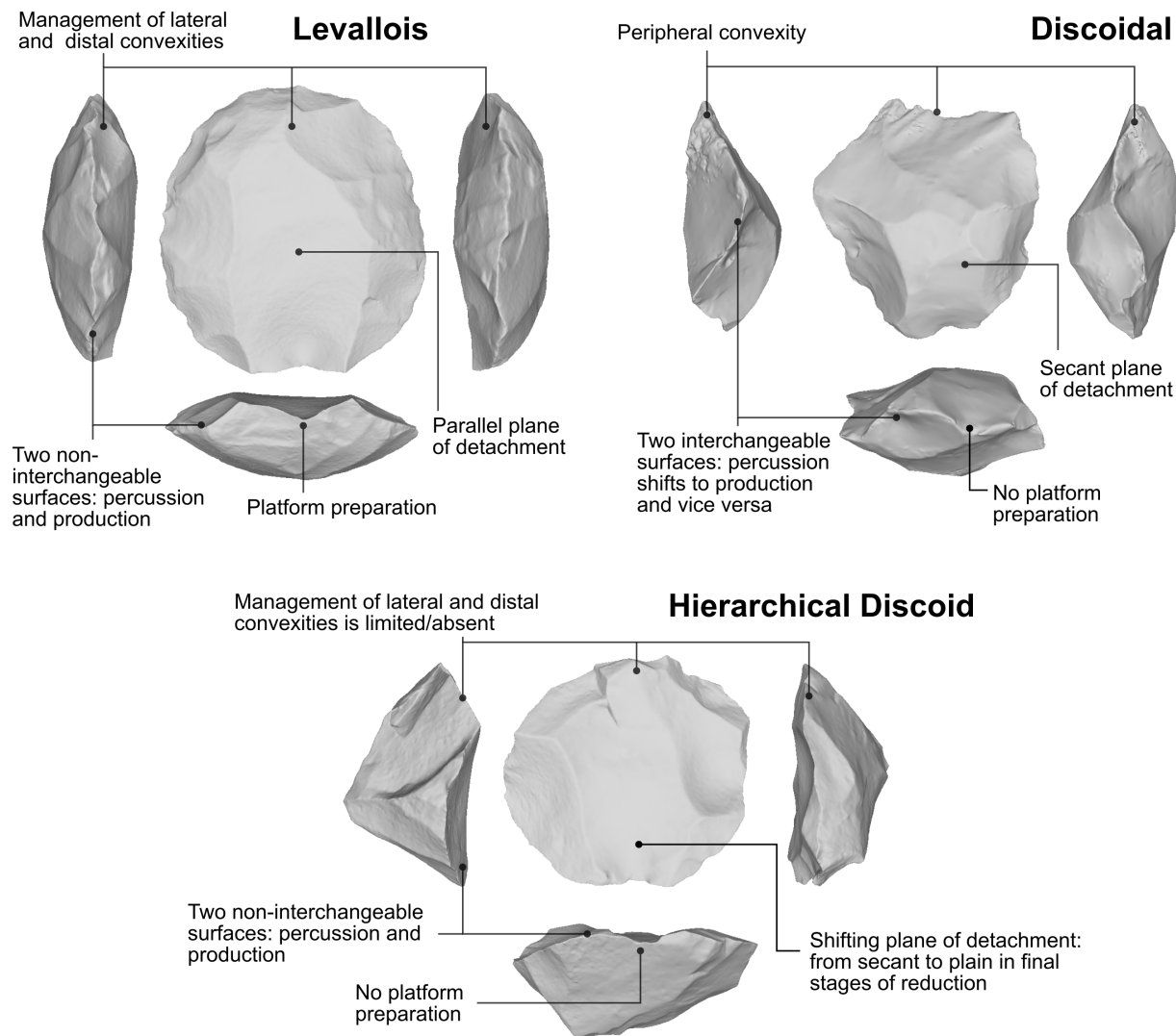


Figure 3: Experimental cores from which flakes included in the present study were detached. Their technological defining features are outlined)

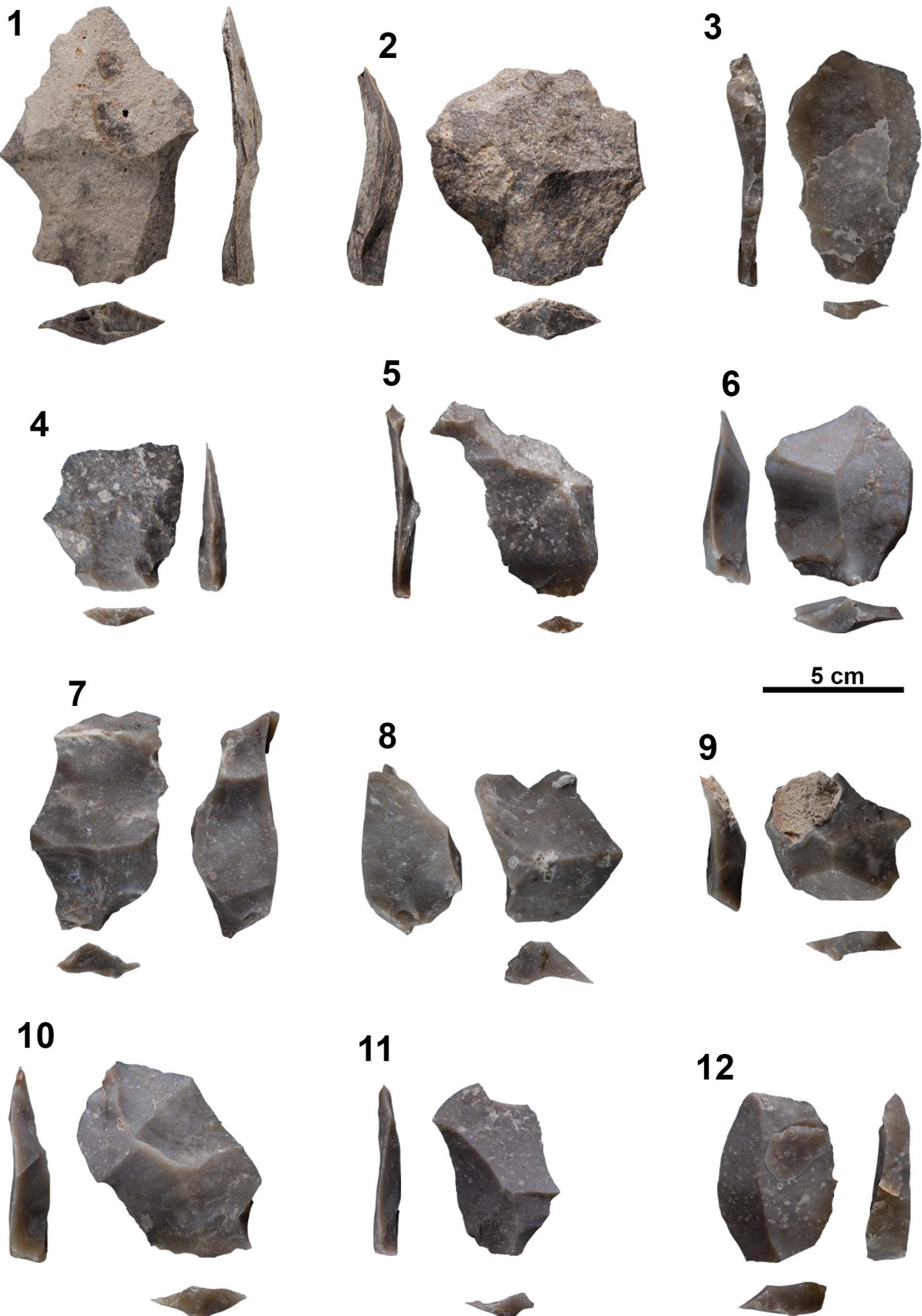


Figure 4: Sample of experimental materials included in this study. 1-5): flakes from Levallois preferential and recurrent centripetal reduction sequences; 6-9) flakes from discoidal reduction sequences; 10-12) flakes from Hierarchical Discoid reduction sequences. (Photographs by M. D. Guillén)

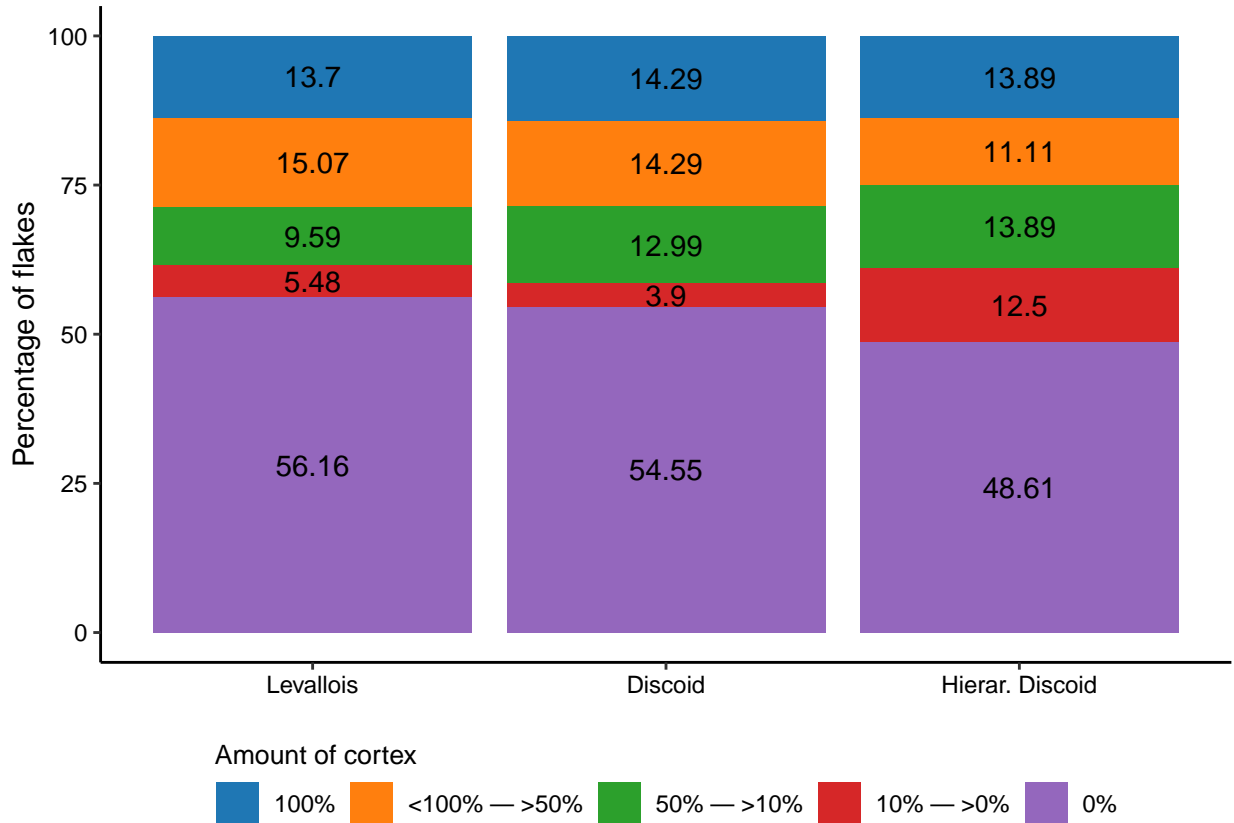
```

geom_bar(stat = "identity") +
ylab("Percentage of flakes") +
ggsci::scale_fill_d3(name = "Amount of cortex",
                      labels = c("100%", "<100% - >50%", "50% - >10%", "10% - >0%", "0%")) +
scale_x_discrete(labels = c("Levallois", "Discoid", "Hierar. Discoid")) +

geom_text(aes(label = (Percentage) %>% round(2)),
          position = position_stack(0.5)) +
theme_classic() +
guides(fill = guide_legend(title.position = "top", nrow = 1)) +
theme(
  axis.text = element_text(color = "black"),
  axis.title.x = element_blank(),
  legend.position = "bottom",
  legend.title = element_text(size = 10, color = "black"),
  legend.text = element_text(size = 9, color = "black"))

```

'summarise()' has grouped output by 'Class'. You can override using the '.groups' argument.



```

# Bagolini scatter plot
ML_Data %>%
  ggplot(aes(Width, Length), color = Class) +
  geom_segment(x = 40, y = 0, xend = 0, yend = 40, color = "gray48") +

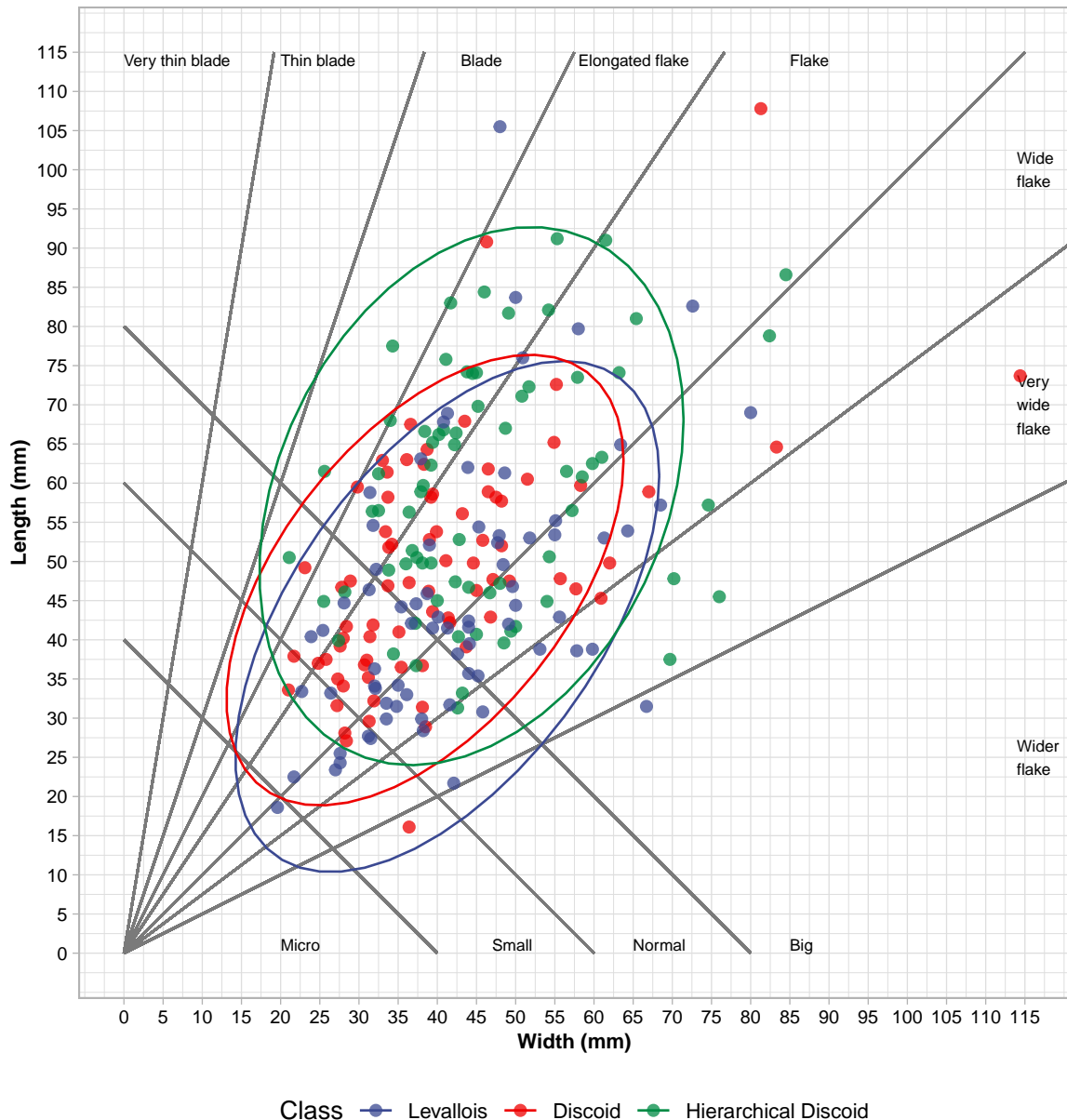
```

```

geom_segment(x = 60, y = 0, xend = 0, yend = 60, color = "gray48") +
geom_segment(x = 80, y = 0, xend = 0, yend = 80, color = "gray48") +
geom_segment(x = 0, y = 0, xend = 115, yend = 115, color = "gray48") +
geom_segment(x = 0, y = 0, xend = (115/6), yend = 115, color = "gray48") +
geom_segment(x = 0, y = 0, xend = (115/3), yend = 115, color = "gray48") +
geom_segment(x = 0, y = 0, xend = (115/2), yend = 115, color = "gray48") +
geom_segment(x = 0, y = 0, xend = (115/1.5), yend = 115, color = "gray48") +
geom_segment(x = 0, y = 0, xend = (115/0.75), yend = 115, color = "gray48") +
geom_segment(x = 0, y = 0, xend = (115/0.5), yend = 115, color = "gray48") +
geom_segment(x = 0, y = 0, xend = 115, yend = (115/2), color = "gray48") +
geom_segment(x = 0, y = 0, xend = 115, yend = 114, color = "gray48") +
geom_segment(x = 0, y = 0, xend = 20, yend = 114, color = "gray48") +
geom_segment(x = 0, y = 0, xend = 43, yend = 114, color = "gray48") +
geom_segment(x = 0, y = 0, xend = 58, yend = 114, color = "gray48") +
geom_segment(x = 0, y = 0, xend = 85, yend = 114, color = "gray48") +
geom_segment(x = 0, y = 0, xend = 114, yend = 100, color = "gray48") +
geom_segment(x = 0, y = 0, xend = 114, yend = 70, color = "gray48") +
geom_segment(x = 0, y = 0, xend = 114, yend = 25, color = "gray48") +
geom_point(aes(color = Class), size = 2, alpha = 0.75) +
scale_x_continuous(breaks = seq(0, 115, 5), lim = c(0, 115)) +
scale_y_continuous(breaks = seq(0, 115, 5), lim = c(0, 115)) +
ylab("Length (mm)") +
xlab("Width (mm)") +
theme_light() +
ggsci::scale_color_aaas(labels = c('Levallois', 'Discoid',
                                    'Hierarchical Discoid')) +
labs(color = "Class") +
stat_ellipse(aes(color = Class)) +
guides(color = guide_legend(nrow = 1, title.position = "left")) +
theme(axis.title = element_text(size = 9, color = "black", face = "bold"),
      axis.text = element_text(size = 7.5, color = "black"),
      legend.position = "bottom") +

```

```
coord_fixed()
```



2.2 Attribute analysis

Attribute analyses were performed for each flake. The variables and indexes listed below were recorded and calculated. Measurements were recorded in mm. Some of the measurements recorded were used in the calculation of additional variables. For example, angle height and maximum flake length were used to calculate flake curvature; width measurements (at 25% and 75% length) were used to calculate the angle of the lateral margins; and thickness measurements were used to calculate the average and standard deviation of thickness. Other variables, such as technological length and width (or the above-mentioned width measurements) were also used to calculate ratios (the elongation and carination index), but their use would introduce a size dependence factor in the training of the models. Therefore, the variables employed in the machine learning model training are underlined. The variables considered were:

- Degree of fracture ([Hiscock 2002](#)): complete, proximal fragment, mesial fragment, distal fragment, marginal fragment and longitudinal fragment. Only complete flakes were further analysed.
- Technological length: measured along the axis perpendicular to the striking platform ([Andrefsky 2005](#)).
- Technological width: measured along the axis perpendicular to the technological width ([Andrefsky 2005](#)).
- Width measured at the 25% length of the flake ([Eren & Lycett 2012](#)).
- Width at the 75% length of the flake ([Eren & Lycett 2012](#)).
- Thickness at the 25% length of the flake ([Eren & Lycett 2012](#)).
- Thickness at the 50% length of the flake ([Eren & Lycett 2012](#)).
- Thickness at the 75% length of the flake ([Eren & Lycett 2012](#)).
- Maximum flake length.
- **Maximum thickness**
- **Average thickness:** the average from the three previous measures of thickness.
- **Standard deviation of thickness.**
- Angle height ([Andrefsky 2005](#)): the height of the flake including its curvature.
- Geometric morphology of the platform as per Muller & Clarkson ([2016](#)): rectangle, triangle, rhombus, trapezoid, and ellipse.
- Measurement “x”, “y” and “z” of the platform according to previous geometric morphologies ([Muller & Clarkson 2016](#)).
- **Platform surface:** calculated using previous geometric morphologies and measurements of x, y and z as in Muller & Clarkson ([2016](#)).
- **Platform depth:** which can correspond to the measurement of y or z depending on the geometric morphology of the platform.
- **Platform width:** which can correspond to the measurement of x or y depending on the geometric morphology of the platform.
- **Profile of the platform:** absence of platform, concave, straight, convex, biangular and *chapeau de gendarme*.
- **Preparation of the platform:** no platform, cortical, plain, dihedral, a pans and prepared (facetted).
- **External Platform Angle (EPA)** measured in degrees with a manual goniometer.
- **Internal Platform Angle (IPA)** measured in degrees with a manual goniometer.
- **Relative amount of cortex present at the dorsal face:** recorded according to its extension on the dorsal surface of the flake ([Andrefsky 2005](#)): cortical (100% cortex), more than 50% of cortex

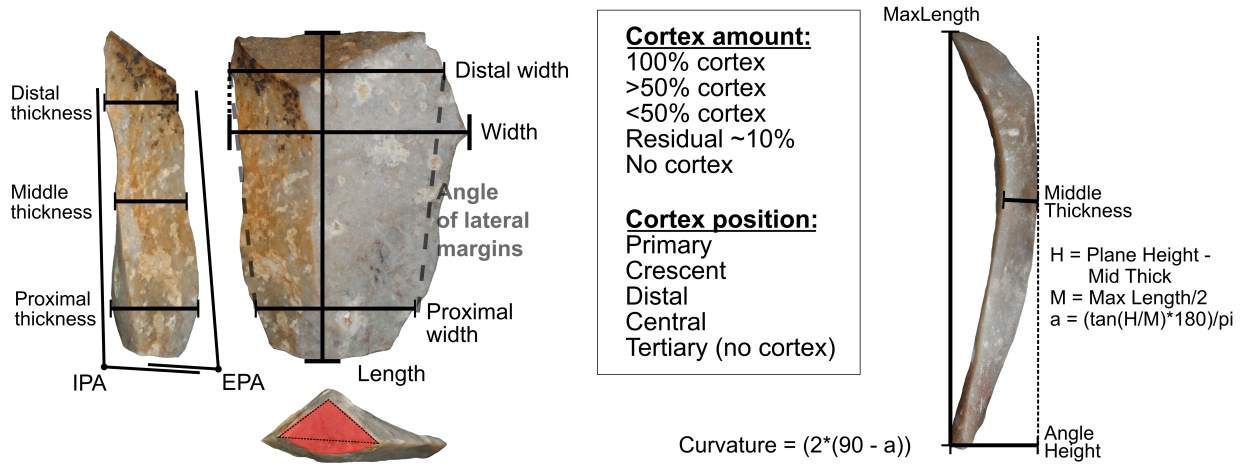


Figure 5: Left: common measures and attributes taken for the analysis of a flake. Right: calculation of flake curvature following Andrefsky (2005)

(excluding cortical flakes), less than 50% of cortex (excluding the following categories), residual presence (<10% and excluding non-cortical flakes), and no cortex.

- **Cortex location:** slightly modified from Marwick (2008), with categories being primary (dorsal surface completely covered by cortex), crescent (cortex located in one of the laterals usually with a crescent shaped form) distal (located at the opposite end of the percussion platform), central (inner part of the flake), and tertiary (no cortex).
- **Number of dorsal scars with length more than 5 mm*.**
- **Number of longitudinal ridges:** individual ridges starting at the platform and reaching the distal part of the flake.
- **Transversal section:** triangular, right-angled triangle, trapezoidal, rectangular trapezoid shape and ovular.
- **Termination type of the flake:** feather, hinge, step or plunging following Cotterell & Kamminga (1987).

Platform morphology	Rectangle	Triangle	Rhombus	Ellipse	Trapezoid
Platform surface	$(x*y)/1.98$	$(x*y)/2$	$(x*y)/2$	$[(x*y)/4] * \pi$	$[(x+y)/2] * z$
Platform width	x	x	x	x	x
Platform depth	y	y	y	y	z

Figure 6: Geometric morphologies employed to measure platform surface, depth and width following Muller & Clarkson (2016)

- **Simplified technological category of flakes:** flake, backed flake (including core edge flake), and pseudo-Levallois point.
- Weight in grams (precision of 0.01).
- **Elongation index:** the quotient of technological length divided by technological width ([Laplace 1968](#)).
- **Crenulated index:** the quotient of length or width (the one with the lowest value) divided by the maximum thicknesses ([Laplace 1968](#)).
- **Angle of the lateral margins:** describes the relationship between the two lateral edges of a flake. Flakes with expanding edges (wider in the distal part) will have negative values, contracting or pointed (wider in the proximal part than in the distal part) artefacts will have positive values, and rectangular artefacts (similar proximal and distal width) will have values near 0 ([Clarkson 2007](#): 37). The angle of the lateral margins is calculated by multiplying by two the value of the reverse tangent of proximal width minus distal with, and dividing the result by two times the maximum length ([Clarkson 2007](#): 38)
- **Flake curvature:** measured in degrees and calculated as described in Andrefsky ([2005](#)). Flakes presenting a 180° curvature are perfectly straight flakes, while decreasing values indicate an increase in curvature.
- **Surface area of the flake:** the product of flake technological width multiplied by its length ([Dibble 1989](#)).
- **Ratio of surface area against thickness:** surface area of the flake divided by average thickness.
- **Ratio of surface area against platform surface:** the quotient of the surface area divided by platform area.

2.3 Machine learning models

The following ten machine learning models were tested for their ability to differentiate between backed flakes extracted from the two surfaces of the core using each knapping method:

- **Linear Discriminant Analysis (LDA):** reduces dimensionality for the purpose of maximising the separation between classes while decision boundaries divide the predictor range into regions ([Fisher 1936; James *et al.* 2013](#)).
- **K-nearest neighbor (KNN):** classifies cases by assigning the class of similar known cases. The 'k' in KNN refers to the number of cases (neighbours) to consider when assigning a class, which must be found by testing different values. Given that KNN uses distance metrics to compute nearest neighbours and that each variable is in different scales, the data must be scaled and centred prior to fitting the model ([Cover & Hart 1967; Lantz 2019](#)).
- **Logistic Regression:** essentially adapts continuous regression predictions to categorical outcomes ([Cramer 2004; Walker & Duncan 1967](#)).
- **Decision tree with C5.0 algorithm:** algorithm: an improvement on decision trees for classification ([Quinlan 1996; Quinlan 2014](#)).
- **Random Forest:** made of decision trees. Each tree is grown from a random sample of the data and variables, allowing for each tree to grow differently and to better reflect the complexity of the data ([Breiman 2001](#)).

- **Generalized Boosted Model** ([Greenwell *et al.* 2019; Ridgeway 2007](#)) implements the gradient boosted machine ([Friedman 2001; Friedman 2002](#)) making it possible to detect learning deficiencies and increase model accuracy for a set of random forests.
- **Supported Vector Machines (SVM)**: fit hyperplanes into a multidimensional space with the objective of creating homogeneous partitions ([Cortes & Vapnik 1995; Frey & Slate 1991](#)). The present study tests SVM with linear, radial and polynomial kernels.
- **Artificial Neural Network (ANN)** with multi-layer perception, it uses a series of hidden layers and error backpropagation for model training ([Rumelhart *et al.* 1986](#)).

2.4 Machine learning evaluation

All models were evaluated by means of a 10x50 k-fold cross validation (10 folds and 50 cycles). Accuracy and area under the curve (AUC) were used as measurements of overall performance for the selection of the best model. ‘Accuracy’ measures the model’s correct predictions against the overall cases provided to the model and can range from 0 to 1. The accuracy of a random classifier is $1/k$ (k being the number of classes). For the present study, the random classifier had an accuracy of 0.33.

The AUC is a measure of performance derived from the receiver operating characteristic (ROC) curve. The ROC curve is used to evaluate the ratio of detected true positives while avoiding false positives ([Bradley 1997; Spackman 1989](#)). The ROC curve makes it possible to visually analyse model performance and calculate the AUC, which ranges from 1 (perfect classifier) to 0.5 (random classifier). The ROC and AUC are commonly applied in two-class problems and their extension to multiclass problems is usually done through pairwise analysis. In the case of the ROC curve, individual curves of each class are plotted using the previously mentioned “one vs all” approach. The present study tested 10 different models with a three-class classification problem which would involve a total of 30 different ROC curves (10 per class in each model). In this paper, we have provided only the three ROC curves of the best model.

The AUC ranges of values are usually interpreted as follows: 1 to 0.9: outstanding; 0.9 to 0.8: excellent or good; 0.8 to 0.7: acceptable or fair; 0.7 to 0.6: poor; and 0.6 to 0.5: no discrimination ([Lantz 2019](#)). When analysing lithic materials, the use of thresholds to guarantee true positives and avoid false positives is of special interest. The use of decision thresholds and derived measures of accuracy (ROC curve and AUC) can be especially useful in lithic analysis since it is expected that products from initial reduction stages are morphologically similar, independent of the knapping method. These products are expected to show a greater mixture between methods and have lower probability values. The use of thresholds better indicates the accuracy of a model considering these probability values.

This study was conducted using an R version 4.1.1 in IDE RStudio version 2021.09.0 ([R. C. Team 2019; Rs. Team 2019](#)). The data and graphs were managed using the tidyverse v.1.3.2 package ([Wickham *et al.* 2019](#)). The LDA and KNN were trained with the MASS (Modern Applied Statistics with S) v.7.3.58.1 package ([Venables & Ripley 2002](#)). The random forest was trained using the ranger v.0.14.1 package ([Wright & Ziegler 2017](#)). The SVM was trained using the e1071 v.1.7.12 package ([Karatzoglou *et al.* 2006; Karatzoglou *et al.* 2004](#)). The RSNNS v.0.4.14 (Stuttgart Neural Network Simulator) package ([Bergmeir & Benítez 2012](#)) was used to train the multi-layer ANN with backpropagation. The k-fold cross validation of all models, precision metrics, and confusion matrix were obtained using the caret v.6.0.93 package ([Kuhn 2008](#)). Machine learning models also provide insights into variable importance for classification. The caret package was used to extract variable importance after each k-fold cross validation (see supplementary information). ROC curves and AUC values are obtained using the package pROC v.1.18.0 ([Robin *et al.* 2011](#)).

2.4.1 Preprocessing for model training Prior to the training the models it is necessary to remove a series of variables such as “Artifact_ID”, “Core”, “Complete”, etc. These variables are employed to ensure the quality of the dataset, but are not employed in model training.

```

# Remove unwanted columns
ML_Data <- ML_Data %>%
  select(-c(Artifact_ID, Core, Complete, Frag_Cat, Knapping_Phase,
            Length, Width, Weight))

# Select character columns and cortex location
x <- colnames(ML_Data) %>%
  select_if(is.character) %>%
  select(Plat_Prof:Flake_Type)

x <- append(x, "Cortex_Loc")

# Only one CG platform. Make into convex
ML_Data$Plat_Prof[ML_Data$Plat_Prof == "CG"] <- "CX"

# Dummy coding of qualitative variables
ML_Data <- fastDummies::dummy_cols(
  ML_Data,
  select_columns = c(x),
  remove_first_dummy = TRUE,
  remove_selected_columns = TRUE)

```

2.4.2 Training of the models The following code sets up 50 cycles of a 10 fold cross validation. Additionally, the final class probabilities for each case are saved.

```

# Set validation
trControl <- trainControl(method = "repeatedcv",
                           verboseIter = TRUE,
                           number = 10,
                           repeats = 50,
                           savePredictions = "final",
                           classProbs = TRUE)

```

The following code trains all the above mentioned models.

```

# LDA Model
set.seed(123)
LDA_Model <- train(Class ~.,
                     ML_Data,
                     method = "lda",
                     trControl = trControl,
                     preProc = c("center", "scale"),
                     metric = "Accuracy",
                     importance = 'impurity')

# KNN model
set.seed(123)
KNN_Model <- train(Class ~.,
                     ML_Data,
                     method = "knn",
                     preProc = c("center", "scale"),
                     trControl = trControl,

```

```

    tuneGrid   = expand.grid(k = 2:30),
    metric = "Accuracy")

# Logistic regression
set.seed(123)
Log_Reg <- train(Class ~.,
                  ML_Data,
                  method = "glmnet",
                  family = 'multinom',
                  preProcess = c("center","scale"),
                  trControl = trControl,
                  metric = "Accuracy",
                  importance = 'impurity')

# C5.0 model
set.seed(123)
C50_Mod <- train(Class ~.,
                  ML_Data,
                  method = "C5.0",
                  trControl = trControl,
                  metric = "Accuracy",
                  importance = 'impurity')

# Random Forest
best_tune <- data.frame(
  mtry = numeric(0),
  Num_Trees = numeric(0),
  Split_Rule = character(0),
  Precision = numeric(0),
  Node.Size = numeric(0))

my_seq <- seq(350, 700, 25)

set.seed(123)
for (x in my_seq){

  RF_Model <- train(Class ~.,
                      ML_Data,
                      method = "ranger",
                      trControl = trControl,
                      tuneGrid =
                        expand.grid(.mtry = seq(1, 10, 1),
                                   .min.node.size = seq(1, 6, 1),
                                   .splitrule = c("gini", "extratrees")),
                      metric = "Accuracy",
                      importance = 'impurity')

  Bst_R <- data.frame(
    mtry = RF_Model$bestTune[[1]],
    Num_Trees = x,
    Split_Rule = RF_Model$bestTune[[2]],
    Precision = max(RF_Model$results[[4]]),

```

```

    Node.Size = RF_Model$bestTune[[3]]
  )

best_tune <- rbind(best_tune, Bst_R)
Bst_R <- c()
}

# Best tune
set.seed(123)
RF_Model <- train(
  frmla,
  PCA_Coord,
  method = "ranger",
  trControl = trControl,
  tuneGrid = expand.grid(
    .mtry = 40,
    .min.node.size = 1,
    .splitrule = "extratrees"),
  num.trees = 550,
  metric = "Accuracy",
  importance = 'impurity')

# GBM
set.seed(123)
Boost_Tree <- train(Class ~.,
  ML_Data,
  method = "gbm",
  trControl = trControl,
  metric = "Accuracy",
  tuneGrid =
    expand.grid(
      n.trees = seq(from = 300, to = 700, by = 50),
      interaction.depth = seq(from = 1, to = 10, length.out = 5),
      shrinkage = 0.1,
      n.minobsinnode = as.integer(seq(1, 10, length = 5)))))

# SVM linear
set.seed(123)
SVM_Linear <- train(Class ~.,
  ML_Data,
  method = "svmLinear",
  preProcess = c("center", "scale"),
  trControl = trControl,
  tuneGrid = expand.grid(C = seq(0.01, 3, length = 20)),
  metric = "Accuracy",
  importance = 'impurity')

# SVM Radial
set.seed(123)
SVM_Radial <- train(Class ~.,
  ML_Data,
  method = "svmRadial",
  preProcess = c("center", "scale"),

```

```

    trControl = trControl,
    tuneGrid =
      expand.grid(C = seq(0.01, 3, length = 20),
                  sigma = seq(0.0001, 1, length = 20)),
    metric = "Accuracy",
    importance = 'impurity')

# SVM Poly
set.seed(123)
SVM_Poly <- train(Class ~.,
                    ML_Data,
                    method = "svmPoly",
                    preProcess = c("center", "scale"),
                    trControl = trControl,
                    metric = "Accuracy",
                    tuneGrid =
                      expand.grid(C = seq(0.01, 3, length = 15),
                                  scale = seq(0.001, 1, length = 15),
                                  degree = as.integer(seq(1, 3, 1))),
                    importance = 'impurity')

# ANN
set.seed(123)
mlp_Mod = train(Class ~.,
                 ML_Data,
                 method = "mlpML",
                 preProc = c('center', 'scale'),
                 trControl = trControl,
                 tuneGrid =
                   expand.grid(
                     layer1 = c(1:8),
                     layer2 = c(0:8),
                     layer3 = c(0:8)))

```

3. Data results

All of the models presented a general accuracy of above 0.6 and far above the random classifier (0.33). The overall model performance indicated that SVM with polynomial kernel provided the best classification metrics for both accuracy and AUC. SVM with polynomial kernel had the best overall accuracy value (0.667) and the best AUC (0.824), an excellent or good value. The SVM with polynomial kernel accuracy value was closely followed by the random forest (0.666) and logistic regression (0.662). The gradient boosting machine model and ANN presented the lowest accuracy values (0.613 and 0.614, respectively). The random forest also presented the second highest AUC value (0.816) followed by SVM with radial kernel (0.815), both values were excellent or good. Again, ANN and the generalised boosted model presented the lowest AUC values (0.772 and 0.795 respectively), although both values can be considered acceptable or fair.

```

# Model performance (accuracy and AUC)
data.frame(
  Model = c("LDA", "KNN", "Log. Reg", "C5.0", "Ran. Forest",
            "Boost. Tree", "SVML", "SVMR", "SVMP", "ANN"),
  Accuracy = rbind(
    round(confusionMatrix(LDA_Model$pred$obs, LDA_Model$pred$pred)$overall['Accuracy'], 3),

```

```

round(confusionMatrix(KNN_Model$pred$obs, KNN_Model$pred$pred)$overall['Accuracy'], 3),
round(confusionMatrix(Log_Reg$pred$obs, Log_Reg$pred$pred)$overall['Accuracy'], 3),
round(confusionMatrix(C50_Mod$pred$obs, C50_Mod$pred$pred)$overall['Accuracy'], 3),
round(confusionMatrix(RF_Final$pred$obs, RF_Final$pred$pred)$overall['Accuracy'], 3),
round(confusionMatrix(Boost_Tree$pred$obs, Boost_Tree$pred$pred)$overall['Accuracy'], 3),
round(confusionMatrix(SVM_Linear$pred$obs, SVM_Linear$pred$pred)$overall['Accuracy'], 3),
round(confusionMatrix(SVM_Radial$pred$obs, SVM_Radial$pred$pred)$overall['Accuracy'], 3),
round(confusionMatrix(SVM_Poly$pred$obs, SVM_Poly$pred$pred)$overall['Accuracy'], 3),
round(confusionMatrix(mlp_Mod$pred$obs, mlp_Mod$pred$pred)$overall['Accuracy'], 3),
AUC = rbind(
  round(pROC::multiclass.roc(LDA_Model$pred$obs, LDA_Model$pred[,4:6])$auc[[1]],3),
  round(pROC::multiclass.roc(KNN_Model$pred$obs, KNN_Model$pred[,4:6])$auc[[1]],3),
  round(pROC::multiclass.roc(Log_Reg$pred$obs, Log_Reg$pred[,6:8])$auc[[1]],3),
  round(pROC::multiclass.roc(C50_Mod$pred$obs, C50_Mod$pred[,7:9])$auc[[1]],3),
  round(pROC::multiclass.roc(RF_Final$pred$obs, RF_Final$pred[,6:8])$auc[[1]],3),
  round(pROC::multiclass.roc(Boost_Tree$pred$obs, Boost_Tree$pred[,8:10])$auc[[1]],3),
  round(pROC::multiclass.roc(SVM_Linear$pred$obs, SVM_Linear$pred[,4:6])$auc[[1]],3),
  round(pROC::multiclass.roc(SVM_Radial$pred$obs, SVM_Radial$pred[,5:7])$auc[[1]],3),
  round(pROC::multiclass.roc(SVM_Poly$pred$obs, SVM_Poly$pred[,6:8])$auc[[1]],3),
  round(pROC::multiclass.roc(mlp_Mod$pred$obs, mlp_Mod$pred[,6:8])$auc[[1]],3)
))

```

	Model	Accuracy	AUC
## 1	LDA	0.629	0.807
## 2	KNN	0.655	0.806
## 3	Log. Reg	0.662	0.813
## 4	C5.0	0.625	0.799
## 5	Ran. Forest	0.666	0.816
## 6	Boost. Tree	0.613	0.795
## 7	SVML	0.637	0.805
## 8	SVMR	0.655	0.815
## 9	SVMP	0.667	0.824
## 10	ANN	0.614	0.772

```

# Performance metrics of SVMP
SVMP.Performance <- data.frame(confusionMatrix(SVM_Poly$pred$pred, SVM_Poly$pred$obs)[[4]])
SVMP.Performance %>%
  select(Sensitivity, Specificity, Precision, F1, Prevalence, Balanced.Accuracy) %>%
  mutate(Class = c("Levallois", "Discoidal", "Hierar. Disc."))

```

	Sensitivity	Specificity	Precision	F1	Prevalence	Balanced.Accuracy
## Class: L	0.7827397	0.9115436	0.8125711	0.7973765	0.3288288	0.8471417
## Class: D	0.6561039	0.8026207	0.6383624	0.6471116	0.3468468	0.7293623
## Class: HD	0.5616667	0.7860000	0.5574855	0.5595683	0.3243243	0.6738333
	Class					
## Class: L	Levallois					
## Class: D	Discoidal					
## Class: HD	Hierar. Disc.					

Classification metrics per class, confusion matrix and ROC along with AUCs of SVM with polynomial kernel exhibited marked differences between knapping methods (Figure 9). In all cases, classification metric values were higher than the no-information ratio (prevalence) of each class (0.329 for Levallois, 0.347 for

discoid and 0.324 for hierarchical discoid). In general, SVM with polynomial kernel best identified products obtained from Levallois preferential and recurrent centripetal reduction sequences. This resulted in a notably high value of sensitivity (0.783) along with a high value of general performance (F1 value of 0.797), and an outstanding AUC value (0.91). While it was slightly more common to erroneously identify Levallois products as hierarchical discoid products (12.44%) than to erroneously identify them as discoid products (9.29%), both values were notably low.

```
# ROC and AUC of each model
MC.ROC <- SVM_Poly$pred %>%
  select(pred, obs, L, D, HD) %>%
  mutate(
    LvsAll = case_when(obs == "D" ~ "Rest",
                        obs == "HD" ~ "Rest",
                        obs == "L" ~ "L"),
    DvsAll = case_when(obs == "D" ~ "D",
                        obs == "HD" ~ "Rest",
                        obs == "L" ~ "Rest"),
    HDvsAll = case_when(obs == "D" ~ "Rest",
                        obs == "HD" ~ "HD",
                        obs == "L" ~ "Rest"))
  
```

```
x <- roc(MC.ROC$LvsAll, MC.ROC$L)
SVMP.ROCs <- data.frame(
  Sensi = x$sensitivities,
  Speci = x$specificities,
  Class = "Levallois")

x <- roc(MC.ROC$DvsAll, MC.ROC$D)
temp <- data.frame(
  Sensi = x$sensitivities,
  Speci = x$specificities,
  Class = "Discoidal")
SVMP.ROCs <- rbind(SVMP.ROCs, temp)

x <- roc(MC.ROC$HDvsAll, MC.ROC$HD)
temp <- data.frame(
  Sensi = x$sensitivities,
  Speci = x$specificities,
  Class = "Hierar. Disc.")
SVMP.ROCs <- rbind(SVMP.ROCs, temp)

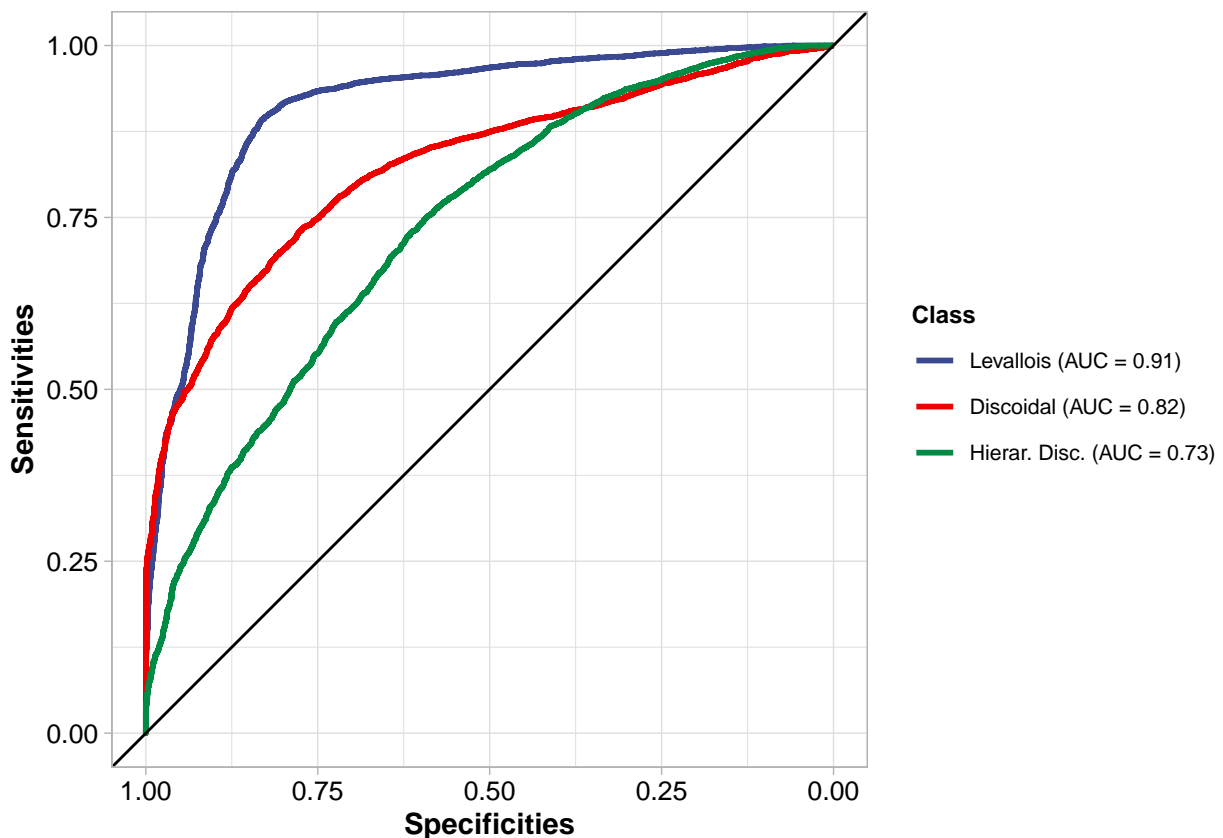
#Set factors (otherwise legend will not correspond)
SVMP.ROCs$Class <- factor(SVMP.ROCs$Class,
                            levels = c(
                              "Levallois",
                              "Discoidal",
                              "Hierar. Disc."))
  
```

```
# Plot the three ROC's and AUC's in legend
SVMP.ROCs %>%
  ggplot(aes(Speci, Sensi, color = Class)) +
  geom_line(size = 1.01) +
  scale_x_continuous(trans = "reverse") +
  
```

```

ggsci::scale_color_aaas(
  labels = c(paste0("Levallois ", "(AUC = ", round(auc(MC.ROC$LvsAll, MC.ROC$L)[[1]], 2), ")"),
             paste0("Discoidal ", "(AUC = ", round(auc(MC.ROC$DvsAll, MC.ROC$D)[[1]], 2), ")"),
             paste0("Hierar. Disc. ", "(AUC = ", round(auc(MC.ROC$HDvsAll, MC.ROC$HD)[[1]], 2), ")"))
) +
  coord_fixed() +
  theme_light() +
  xlab("Specificities") +
  ylab("Sensitivities") +
  geom_abline(intercept = 1, slope = 1) +
  theme(
    legend.title = element_text(color = "black", face = "bold", size = 9),
    legend.text = element_text(color = "black", size = 8),
    axis.text = element_text(color = "black", size = 10),
    axis.title = element_text(color = "black", size = 11, face = "bold"))

```



```

## Confusion matrix of SVMP
# Obtain from caret and reshape
SVM_Poly.Confx <- confusionMatrix(SVM_Poly)$table
SVM_Poly.Confx <- reshape2::melt(SVM_Poly.Confx)

# Normalize the data
SVM_Poly.Confx <- SVM_Poly.Confx %>% mutate(
  value = case_when(
    Reference == "L" ~ (value/sum(confusionMatrix(SVM_Poly)$table[1:3]))*100,
    Reference == "D" ~ (value/sum(confusionMatrix(SVM_Poly)$table[4:6]))*100),
  Reference)

```

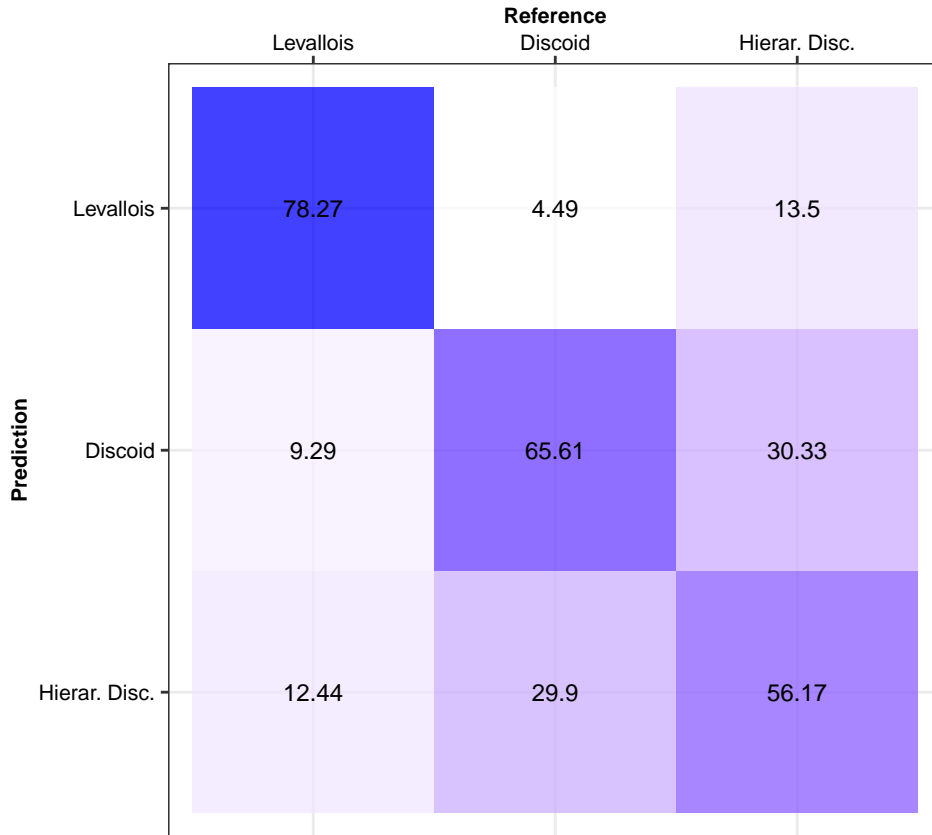
```

    Reference == "HD" ~ (value/sum(confusionMatrix(SVM_Poly)$table[7:9])*100),
  )
)

# Set factors and labels of reference and prediction
SVM_Poly.Confx$Prediction <- factor(SVM_Poly.Confx$Prediction,
                                      levels = c("HD", "D", "L"),
                                      labels = c(
                                        "Hierar. Disc.", "Discoid", "Levallois"))
SVM_Poly.Confx$Reference <- factor(SVM_Poly.Confx$Reference,
                                      levels = c("L", "D", "HD"),
                                      labels = c(
                                        "Levallois", "Discoid", "Hierar. Disc."))

# Plot confusion matrix
SVM_Poly.Confx %>%
  ggplot(aes(Reference, Prediction, fill = value)) +
  geom_tile(alpha = 0.75) +
  geom_text(aes(label = round(value, 2)), size = 3) +
  scale_fill_gradient(low = "white", high = "blue") +
  scale_x_discrete(position = "top") +
  theme_bw() +
  coord_fixed() +
  theme(legend.position = "none",
        axis.title = element_text(size = 8, color = "black", face = "bold"),
        axis.text = element_text(size = 7.5, color = "black"),
        title = element_text(size = 8, color = "black", face = "bold"))

```



Products from discoid bifacial reduction sequences were the second best identified by the SVM with polynomial kernel. While a notable confusion occurred between discoid and hierarchical discoid products, the F1 general performance value (0.647) was still quite high, and the AUC value was found to be excellent or good (0.82). The confusion matrix (Figure 7) shows that the erroneous identification of products from discoid reduction sequences is due to confusion with products resulting from the hierarchical discoid method (29.9%), while their misclassification as Levallois is residual (4.49%). Hierarchical discoid products yielded the lowest values of classification metrics. The general performance metric F1 had a value of 0.56 and relatively low values of sensitivity (0.562) and precision (0.557). Despite these relatively low values, the AUC for the hierarchical discoid products was still acceptable or fair (0.73), which indicates that the application of decision thresholds can support and improve the identification of products from hierarchical discoid reduction sequences. These low classification metrics were clearly related to the SVM with polynomial kernel mistaking hierarchical discoid products as discoid products, along with a residual although notable confusion with Levallois products (13.5%).

The importance of the discriminating variables differed for each knapping method. Figure 10 presents the discriminating variables whose importance values exceeded 50 for each knapping method. For Levallois products, the most important discriminating variables related to ratios of flake size to thickness (the carination index was the most important, and the flake surface to thickness ratio was also considered highly important), thickness (mean and maximum thickness), and platform angle (with IPA having a slightly higher value than EPA). Qualitative attributes such as type of platform were also considered important for the discrimination of Levallois products. Plain and prepared platforms had importance values of 72.19 and 71.19, respectively. The selection of variables for the identification of discoid products was similar to those for Levallois, although with differences in the order of importance. As with the Levallois, the carination index was considered the most important variable, while both measures of platform angle (IPA and EPA) were considered the second and third most important variables. Similar to the Levallois products, measures of thickness and platform type were also considered important in the identification of discoid products.

Discriminating hierarchical discoid products proved to be more complex, with none of the variables reaching the maximum value. The SVM with polynomial kernel model considered thickness measurements (maximum and mean thickness) along with platform angle measurements (EPA and IPA) as the most important variables for the discrimination of hierarchical discoid products. The carination index was considered a much less important measurement (value of 77.18) compared to its importance for the identification of Levallois and discoid products.

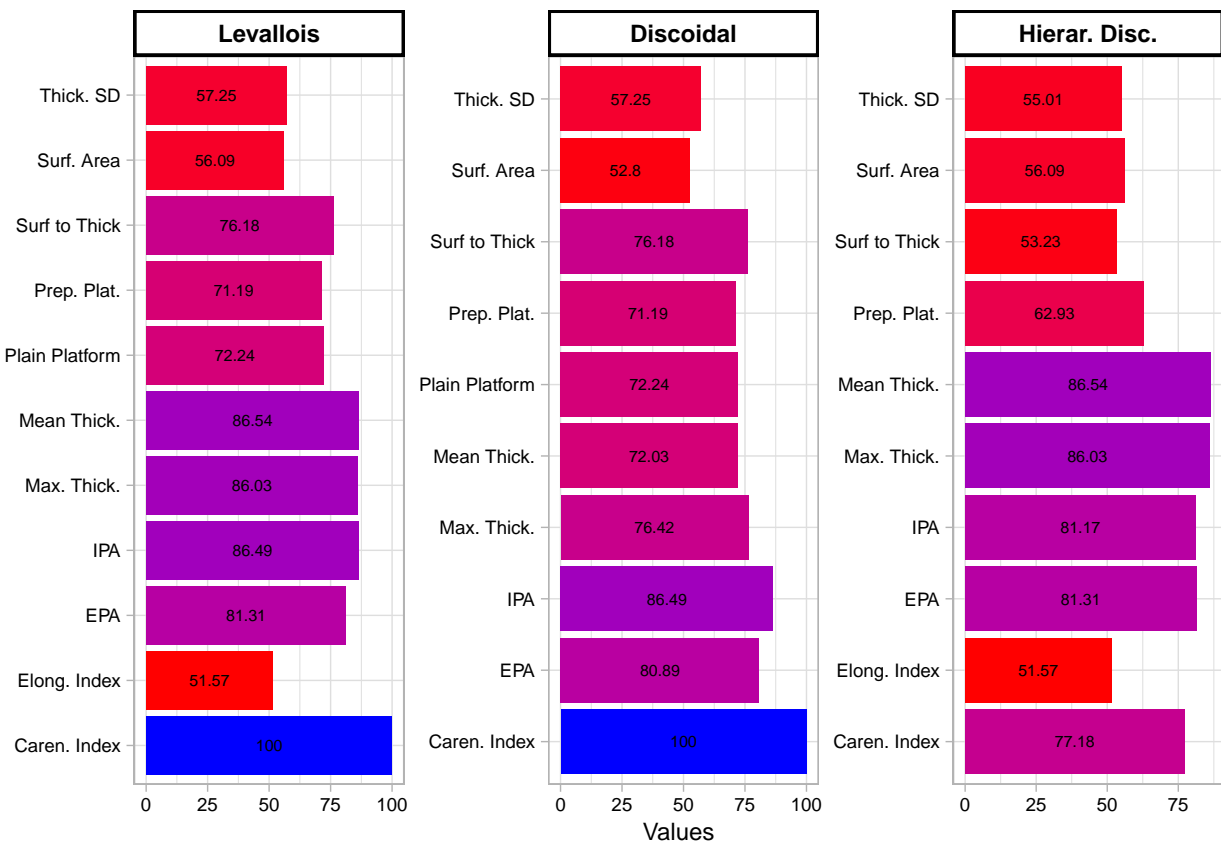
An additional variable which ranked slightly above the importance value threshold is the standard deviation of thickness. Standard deviation of thickness presented importance values of 57.25 for Levallois and discoid products, and 55.01 for hierarchical discoid products. Thus, although it is not a key variable for discrimination, differences can be observed in the thickness variations between products of the different knapping methods. For both Levallois and discoid products, the IPA was a slightly better discriminatory variable than EPA. For hierarchical discoid products, the EPA had a slightly higher (81.31) discriminatory value than IPA (81.17). This indicates that IPA tends to be a better discriminating variable for the identification of knapping methods.

```
## Variable importance
# Data frame of PC importance
tibble(
  Variable = rownames(varImp(SVM_Poly, sale = TRUE)$importance),
  Importance.L = varImp(SVM_Poly, sale = TRUE)$importance[, 1],
  Importance.D = varImp(SVM_Poly, sale = TRUE)$importance[, 2],
  Importance.HD = varImp(SVM_Poly, sale = TRUE)$importance[, 3]) %>%
  mutate(Variable = c(
    "Elong. Index", "Mean Thick.", "Max. Thick.", "Caren. Index", "Surf. Area",
    "Surf to Thick", "Angle Lat. Marg.", "Thick. SD", "CV Thick.", "Curvature",
    "Plat. Surface", "Plat. Depth", "Plat. Width", "Flake Surf. to Plat",
    "Cortex", "No of Scars", "No of Long Ridges", "EPA", "IPA", "X to W ratio",
    "IE to PS", "Surf. to Proximal Width", "CC Platform", "Cx Platform",
    "Straight Plat.", "Dihed. Plat.", "Plain Platform", "Prep. Plat.",
    "Hinge Ter.", "Plunging Term.", "Trap. Section", "Trap. Asy. Section",
    "Tri. Sect.", "Trian. Assym", "Flake", "pL-p", "Crescent Cortex",
    "Distal Cortex", "Center Cortex", "0% Cortex")) %>%
  pivot_longer(cols = Importance.L:Importance.HD,
               names_to = "Importance.Per.Class",
               values_to = "Values") %>%
  filter(Values > 50) %>%
  ggplot(aes(Variable, Values, fill = Values)) +
  geom_bar(stat= "identity", position = "dodge") +
  theme_light() +
  facet_wrap(~ factor(Importance.Per.Class,
                      levels = c("Importance.L",
                                 "Importance.D",
                                 "Importance.HD")),
             labels = c(
               "Levallois",
               "Discoidal",
               "Hierar. Disc.")),
  scale = "free",
  ncol = 3) +
  scale_fill_gradient(low = "red", high = "blue") +
  guides(fill = "none") +
```

```

xlab(NULL) +
coord_flip() +
geom_text(aes(label = round(Values, 2)),
          position = position_stack(vjust = 0.5), size = 2) +
theme(
  axis.text.y = element_text(color = "black", size = 7),
  axis.text.x = element_text(color = "black", size = 7, angle = 0),
  axis.title.x = element_text(color = "black", size = 9),
  axis.title.y = element_text(color = "black", size = 9),
  strip.text = element_text(color = "black", face = "bold", size = 9),
  strip.background = element_rect(fill = "white", colour = "black", size = 1))

```



The analysis of class probabilities based on the reduction sequence and amount of cortex revealed a series of tendencies. Products detached by means of Levallois reduction sequences had the highest mean probability (0.657) of belonging to their true class, independent of cortex amount. This high average can be clearly related to the F1 and AUC measurements. Products detached using Levallois reduction sequences showed a clear tendency: as the cortex amount decreased, the probability of correctly being identified as Levallois increased. This resulted in increased average values of correctly being identified as Levallois: products with 100% cortical flakes had an average of 0.558, > 50% cortex an average of 0.572, < 50% cortex an average of 0.717 and flakes with residual cortex an average of 0.726. A decrease in the average value (0.686) was observed in the case of flakes with no cortex. This decrease in the mean value can be attributed to the fact that this was the most abundant category and included a long tail in the distribution of values as a result of flakes with low probability values of belonging to Levallois reduction sequences. Nevertheless, most of the Levallois reduction sequence flakes were concentrated above a 0.75 probability value.

```

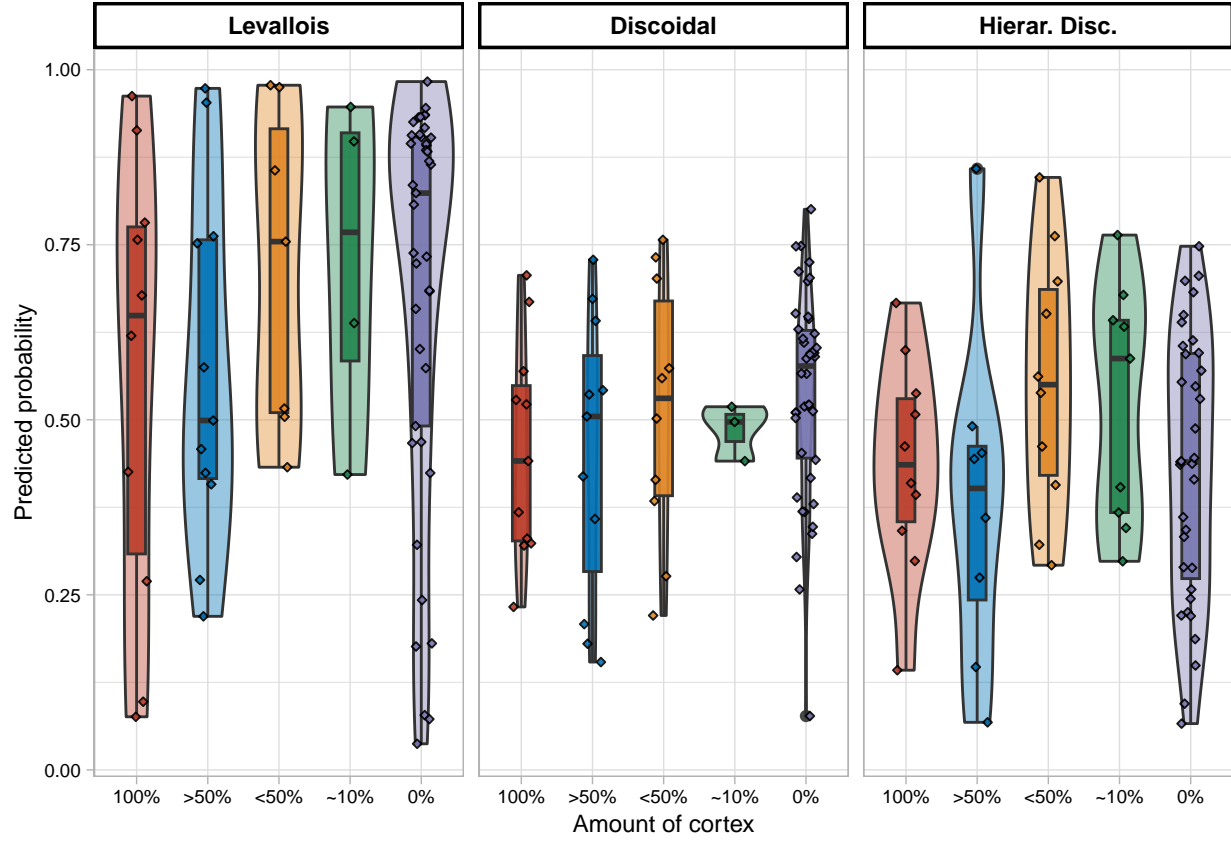
## Compute class probs according to cortex amount #####
# Get probabilities
Cortex.Class <- as.data.frame(SVM_Poly$pred[,4:9]) %>%
  group_by(rowIndex) %>%
  summarise(
    L = mean(L),
    D = mean(D),
    HD = mean(HD))

# Left join
ML_Data$rowID <- 1:nrow(ML_Data)

Cortex.Class <- left_join(Cortex.Class, ML_Data,
                           by = c("rowIndex" = "rowID"))

# Get values for true class
Cortex.Class %>% mutate(
  True.Class.Val = case_when(
    Class == "L" ~ L,
    Class == "D" ~ D,
    Class == "HD" ~ HD
  )) %>%
# and plot
ggplot(aes(factor(Cortex), True.Class.Val, fill = factor(Cortex))) +
  facet_wrap(~ factor(Class,
                       labels =
                         c("Levallois", "Discoidal", "Hierar. Disc."))) +
  geom_violin(alpha = 0.4) +
  geom_boxplot(alpha = 0.9, width = 0.25) +
  ggsci::scale_fill_nejm(
    name = "Cortex amount",
    labels = c(
      "100% Cortical", ">50% Cortical", "<50% Cortical",
      "~10% Cortical", "No Cortex")) +
  ylab("Predicted probability") +
  xlab("Amount of cortex") +
  scale_x_discrete(labels = c("100%", ">50%", "<50%", "~10%", "0%")) +
  geom_jitter(width = 0.15, alpha = 0.9, size = 0.9, shape = 23, aes(fill = factor(Cortex))) +
  theme_light() +
  guides(fill = guide_legend(title.position = "top", nrow = 1)) +
  theme(
    legend.position = "none",
    strip.text = element_text(color = "black", face = "bold", size = 9),
    strip.background = element_rect(fill = "white", colour = "black", size = 1),
    axis.text = element_text(color = "black", size = 7),
    axis.title = element_text(color = "black", size = 9))

```



Products detached from discoid reduction sequences had the second highest average of belonging to their class without considering cortex amount (0.508). As with Levallois products, as the cortex amount decreased, the probability of correctly being attributed to discoid reduction sequences increased. However, this increase was not as marked or clear as for Levallois products. The 100% cortical flakes had an average of 0.456, > 50% cortical flakes an average of 0.45, < 50% cortical an average of 0.512, residual cortical flakes an average of 0.486, and non-cortical flakes an average of 0.538. Again, the distribution of non-cortical flakes presented a long tail of low values, although most of the flakes were concentrated above the 0.5 value.

No clear pattern in the probability distribution of values was observed for the hierarchical discoid flakes. Flakes produced by means of the hierarchical discoid method presented the lowest average probability value of correctly being assigned to their true class (0.456) as expected from the corresponding F1 and AUC values. Flakes with less than 50% cortex and residual cortical flakes had the highest probability averages of correctly being identified as hierarchical discoid flakes (0.554 with less than 50% cortex, and 0.524 with only a residual presence of cortex). However, their low number should be taken into consideration. Non-cortical flakes exhibited the lowest average of probability value (0.432) with a wide range of distribution of probability values, which indicates the difficulty of differentiating even advanced reduction products from hierarchical discoid knapping sequences.

4. Discussion

An analysis of machine learning model performance metrics (accuracy and AUC) found that SVM with polynomial kernel is the best model for differentiating between the three knapping strategies studied. SVM with polynomial kernel provided a general excellent or good AUC value (0.824) and notable accuracy 0.667. However, depending on the knapping strategy, notable differences were found in per-class classification metrics and AUCs. Our results also provide insight into variable importance, showing that measures of flake surface in relation to thickness (carination index and ratio of flake surface to thickness), angle of detachment

(IPA and EPA), and thickness (mean and maximum thickness) are key considerations in the discrimination of knapping methods. In general, we found that corticality affects the ability of the model to determine the knapping method by which the flakes were detached. We detected a general trend: as the amount of cortex diminishes, it becomes easier for the model to identify the knapping method by which the flake was detached. However, again, this trend exhibited marked differences between knapping methods. It was very clear in the case of products detached from Levallois reduction sequences but not so evident for products detached by means of hierarchical discoid reduction sequences.

Flakes detached from Levallois reduction sequences yielded the best identification values, with an individual outstanding AUC (0.91) and high general performance metrics, such as the F1 score (0.797). These results underscore the singularity of products obtained from Levallois preferential and recurrent centripetal reduction sequences and the unlikelihood of confusing them with flakes detached by means of either discoid or hierarchical discoid reduction sequences.

Interpreting the relationship between the discoid and hierarchical discoid methods is more complex. The individual AUC for the identification of discoid flakes offered an excellent or good value (0.82) along with a relatively good F1 score (0.647). These values were not the result of over-predicting the discoid class (35.65% of the assemblage was predicted to be discoid against an actual 34.7%), but rather due to very limited confusion with Levallois products (only 4.49% of cases). As previously mentioned, although the identification of flakes detached by means of hierarchical discoid reduction sequences presented a relatively low F1 score (0.56), it did have an acceptable or fair AUC (0.73). These results indicate the ability of the model to differentiate between the products of the two strategies, reinforcing the notion that they are two different individual technical systems. However, the evaluation of directions of confusion showed that the SVM with polynomial kernel commonly misidentified products from both knapping methods. This can be interpreted as evidence of a very close relationship between the two technical systems.

The relationships between the Levallois, discoid and hierarchical discoid knapping methods have been previously noted by different authors. Lenoir & Turq (1995) proposed the use of the term ‘recurrent centripetal’ to include both discoid debitage and recurrent centripetal Levallois, and that Levallois (*sensu stricto*) should be limited to preferential and recurrent lineal modalities. Similarly, Casanova *et al.* (2014) proposed including Levallois recurrent centripetal and hierarchical discoid modalities within the ‘bifacial centripetal hierarchical’ category. In the present study, the combined use of attribute analysis and machine learning models effectively separated flakes obtained from Levallois recurrent centripetal and preferential sequences from those obtained from hierarchical discoid sequences. A limited percentage of hierarchical discoid products were identified as coming from Levallois recurrent and preferential reduction sequences (13.5%) and the confusion in the opposite direction was less common (12.44). Thus, these results do not support grouping Levallois recurrent centripetal and hierarchical discoid into the same category, as the products from these two approaches seem to be easily differentiated. Mourre (2003) situated the hierarchical discoid knapping method at the margins of the discoid group, given the specific characteristics of the two techniques. At the same time, Levallois recurrent centripetal modality (Mourre 2003) was placed within the Levallois group, but also overlapping with the discoid and hierarchical discoid knapping methods. The results of this study offer a point of agreement and a point of disagreement with this interpretation of the relationships between the three knapping methods. As point of disagreement, the very limited misidentification of discoid and Levallois products does not support the notion of an overlap between these two methods. This high level of separation between Levallois recurrent centripetal and discoid products is also supported by previous studies that used attribute analysis and machine learning models (González-Molina *et al.* 2020). As point of agreement, the notable confusion in the identification of discoid and hierarchical discoid products supports the proposal that the two methods belong to centripetal debitage systems, although our results indicate that a notable level of separation between products from the two systems can be achieved.

Archer *et al.* (2021) used 3D geometric morphometrics for the identification of three distinct knapping methods (laminar, discoid and Levallois) and indicated a general success rate of between 73% and 77%, with Levallois flakes exhibiting the highest identification rate (87%) and discoid flakes the lowest (40%). The overall higher precision reached by Archer *et al.* (2021) was also expected in this study, as we included two classes which are commonly considered to belong to the same family and difficult to differentiate (discoid and hierarchical discoid) instead of three discrete knapping methods. However, their results for the identification

of discoid products contrast with the results of the present study, which yielded notably higher values of sensitivity (0.656) and F1 (0.647) for discoid products. Again, it is important to consider that these moderate values resulted from the inclusion of a closely related strategy (hierarchical discoid) and that confusion with Levallois flakes was minimal. González-Molina *et al.* (2020) presented a balanced dataset of discoid and Levallois recurrent centripetal flakes and tested a series of machine learning algorithms for classification, and found that random forest provided the best results. González-Molina *et al.* (2020) reported 90% precision for the model when the technological classification variable was included for flakes. As they correctly state (González-Molina *et al.* 2020), this variable depends completely on the researcher. Several researchers have called attention to the subjective nature of using the classification “Levallois flake” or the inclusion of the category of “Atypical Levallois flake” (Debénath & Dibble 1994; Hovers 2009). González-Molina *et al.* (2020) additionally provided a random forest model without the technological classification feature which had a precision rate of 80%. In this model, the first five variables were related to flake width. However, aspects of flake width and length can be influenced by initial core and nodule size or by the process of retouch (Shott & Seeman 2017), making them a less desirable variable for the identification of knapping methods.

SVM with polynomial kernel selected variables for knapping method classification already noted in previous studies (Bourguignon 1997; Carmignani *et al.* 2017; González-Molina *et al.* 2020; Mourre 2003; Slimak 2003). The carination index (Laplace 1968) was considered the most important variable for the discrimination of discoid and Levallois products, and also considered notably important for the identification of flakes detached by means of hierarchical discoid reduction sequences. Although thickness measurements are metric variables, they are less subject to variations due to initial nodule and core size or retouch. Previous researchers have highlighted the importance of blank thickness for the differentiation of knapping methods and have shown that Levallois blanks tend to be thinner and more regular than flakes from discoid production systems (Boëda 1994; Boëda 1995b; Bourguignon 1997; González-Molina *et al.* 2020; Lenoir & Turq 1995; Mourre 2003; Slimak 2003; Terradas 2003).

Internal platform angle (IPA) is considered a slightly more important feature than the external platform angle (EPA) for the determination of knapping methods. Previous studies have called attention to the importance of angular relations between the platform and dorsal or ventral surfaces for the discrimination of knapping methods (Boëda 1993; Boëda 1995b; Kelly 1954; Lenoir & Turq 1995; Terradas 2003; Soriano & Villa 2017). In the experimental sample used in this study, Levallois products had IPAs with lower values than those of discoid or hierarchical discoid products, despite the inclusion of cortical elements. Problems with the manual recording of IPA and EPA related to the general morphology of flakes have been acknowledged by other authors (Davis & Shea 1998; Dibble & Pelcin 1995); however, our research emphasises its importance for the determination of knapping methods.

This study highlights the type of platform (prepared and plain platforms) as a key variable for the differentiation of knapping methods. Previous studies have also pinpointed the importance of platform preparation for the differentiation of knapping strategies (Lenoir & Turq 1995). Although this seems to be a significant feature, it is important to consider that platforms vary widely in the archaeological record. For example, Levallois products commonly exhibit plain platforms (Bordes 1961b). Additionally, platform preparation can be related to the knapping style and preferences of the individual knapper, with different knappers producing very similar products with different platform preparation (Driscoll & García-Rojas 2014). Mean thickness of the blank was considered as a key feature by the random forest algorithm, as did the other algorithms tested, along with maximum thickness for the differentiation of knapping methods.

The present study did not include other flaking strategies common in western Europe during the Middle and early Middle Palaeolithic, such as Quina and SSDA (Bourguignon 1997; Forestier 1993). Although in western Europe the coexistence of Levallois and discoid knapping methods with other knapping methods in the same archaeological levels is a subject of debate (Faivre *et al.* 2017; Grimaldi & Santaniello 2014; Marciani *et al.* 2020; Ríos-Garaizar 2017), the present research can be considered for assemblages where Levallois and discoid and hierarchical discoid knapping strategies coexist. Thus, the examination and evaluation of the chaîne opératoire along with the assemblage context and integrity are fundamental for the study of lithic technology (Soressi & Geneste 2011). The chaîne opératoire and assemblage context should be considered prior to the application of machine learning models for the identification of knapping methods.

5.1 Conclusions

The present study used attribute analysis to identify three knapping methods (Levallois, discoid, and hierarchical discoid) in flakes produced with those methods. A secondary objective was to evaluate the degree of confusion between Levallois recurrent centripetal and hierarchical discoid flakes. This secondary objective is relevant since several sites report similar reduction strategies under an umbrella of terms (recurrent centripetal debitage, non-Levallois debitage with hierarchised surfaces, hierarchical bifacial centripetal, centripetal character with preferential surfaces, hierarchical centripetal), which are here grouped under the term hierarchical discoid.

Results from the best machine learning model (SVM with polynomial kernel) indicate that flakes from Levallois recurrent centripetal reduction sequences are highly distinguishable from those of hierarchical discoid reduction sequences. This underscores the singularity of the Levallois reduction strategy, even in its recurrent centripetal modality. Despite some confusion in the identification of flakes detached from discoid and hierarchical discoid reduction sequences, a notable degree of separation can be achieved. This can be considered an indication that the two strategies are separate reduction strategies with their own singularities, while also falling under the umbrella of centripetal strategies.

This study also employed ROC curves and AUCs to identify knapping strategies among flakes. The use of AUCs as a metric of model performance should be taken into consideration in lithic studies that employ machine learning models. This is because they make use of decision thresholds which will sort between ambiguous flakes (such as the ones belonging to initial reduction sequences) and diagnostic flakes (such as the ones from full production). Finally, it is important to highlight that these results illustrate the applicability of machine learning models (along with the present dataset) to contexts of the archaeological record in which these reduction strategies are present.

Acknowledgements

The authors wish to thank the editor and the two anonymous reviewers for their comments and suggestions. This research has been possible thanks to the Program for the Requalification of the University System Margarita Salas (CA1/RSUE/2021-00743) financed through the Spanish “Recovery, Transformation and Resilience Plan” and managed from the Ministry of Universities (Ministerio de Universidades) and the Autonomous University of Madrid (Universidad Autónoma de Madrid). This article is the result of the research project PID2019-103987GB-C33, “En los límites de la diversidad: comportamiento Neandertal en el centro y sur de la Península Ibérica” financed by Agencia Estatal de Investigación (AEI) and Fondo Europeo de Desarrollo Regional (FEDER). This study was also supported by project PID2019-103987GB-C31 from the Spanish Ministry of Science and Innovation (MICINN). Development of the experimentation and analysis of the materials were undertaken at the Laboratory of Experimental Archaeology (Universidad Autónoma de Madrid). The research technical support of María Dolores Guillén was supported by the Spanish Ministry of Science and Innovation through the “María de Maeztu” excellence accreditation (CEX2019-000945-M).

References

- Andrefsky, W. 2005, *Lithics Macroscopic Approaches to Analysis*, Second., (G. Barker, Ed.), Cambridge, Cambridge University Press.
- Archer, W., Djakovic, I., Brenet, M., Bourguignon, L., Presnyakova, D., Schlager, S., Soressi, M. & McPherron, S.P. 2021, Quantifying differences in hominin flaking technologies with 3D shape analysis, *Journal of Human Evolution*, 150: 102912. doi:[10.1016/j.jhevol.2020.102912](https://doi.org/10.1016/j.jhevol.2020.102912)
- Baena, J., Carrión, E., Ruiz, B., Ellwood, B., Sesé, C., Yravedra, J., Jordá, J., Uzquiano, P., Velázquez, R., Manzano, I., Sanchez-Marco, A. & Hernández, F. 2005, Paleoecología y comportamiento humano durante el Pleistoceno Superior en la comarca de Liébana: La secuencia de la Cueva de El Esquilleu (Occidente de Cantabria, España), In: *Neandertales Cantábricos. Estado de la Cuestión* (R. Montes Barquín, Ed.), Monografías., Santander, Museo de Altamira: p. 461–487.
- Bagolini, B. 1968, Ricerche sulle dimensioni dei manufatti litici preistorici non ritoccati, *Annali dell'Università di Ferrara : nuova serie*, 1(10): 195–219.

- Bergmeir, C. & Benítez, J.M. 2012, Neural Networks in R using the Stuttgart Neural Network Simulator: RSNNS, *Journal of Statistical Software*, 46(7). doi:[10.18637/jss.v046.i07](https://doi.org/10.18637/jss.v046.i07)
- Bisson, M.S. 2000, Nineteenth Century Tools for Twenty-First Century Archaeology? Why the Middle Paleolithic Typology of François Bordes Must Be Replaced, *Journal of Archaeological Method and Theory*, 7(1): 1–48. doi:[10.1023/A:10225369000300001](https://doi.org/10.1023/A:10225369000300001) \$18.00/0
- Boëda, E. 1995a, Caractéristiques techniques des chaînes opératoires lithiques des niveaux micoquiens de Külna (Tchécoslovaquie), *Paléo*, 1: 57–72. doi:[10.3406/pal.1995.1380](https://doi.org/10.3406/pal.1995.1380)
- Boëda, E. 1990, De la surface au volume. Analyse des concéptions des débitages Levallois et laminaire, In: *Paleolithique moyen recent et Paleolithique supérieur ancien en Europe. Ruptures et transitions: Examen critique des documents archéologiques* (C. Farizy, Ed.), Mémoires du Musée de Préhistoire d'Ile-de-France., Nemours, A.P.R.A.I.F.: p. 63–68.
- Boëda, E. 1994, *Le concept Levallois: Variabilité des méthodes*, CNRS.
- Boëda, E. 1993, Le débitage discoïde et le débitage Levallois récurrent centripète, *Bulletin de la Société Préhistorique Française*, 90(6): 392–404. doi:[10.3406/bfsp.1993.9669](https://doi.org/10.3406/bfsp.1993.9669)
- Boëda, E. 1995b, Levallois: A Volumetric Construction, Methods, A Technique, In: *The Definition and Interpretation of Levallois Technology* (H. L. Dibble & O. Bar-Yosef, Eds.), Monographs in World Archaeology., Madison, Wisconsin, Prehistory Press: p. 41–68.
- Boëda, E., Geneste, J.-M. & Meignen, L. 1990, Identification de chaînes opératoires lithiques du Paléolithique ancien et moyen, *Paléo*, 2: 43–80.
- Bordes, F. 1953, Levalloisien et Moustérien, *Bulletin de la Société préhistorique de France*, 50(4): 226–235. doi:[10.3406/bfsp.1953.3035](https://doi.org/10.3406/bfsp.1953.3035)
- Bordes, F. 1961a, Mousterian Cultures in France, *Science*, 134(3482): 803–810.
- Bordes, F. 1961b, *Typologie du Paléolithique ancien et moyen*, Bordeaux, CNRS Editions.
- Bourguignon, L. 1996, La conception du débitage Quina, *Quaternaria Nova*, 6: 149–166.
- Bourguignon, L. 1997, *Le Moustérien de type Quina: Nouvelle Définition d'une entité technique*, PhD thesis, Nanterre, Université de Paris X - Nanterre.
- Bourguignon, L. & Turq, A. 2003, Une chaîne opératoire de débitage discoïde sur éclat du Moustérien à denticulés aquitain: Les exemples de Champ Bossuet et de Combre Grenal c.14, In: *Discoid Lithic Technology. Advances and Implications* (M. Peresani, Ed.), BAR International Series., Oxford: p. 131–152.
- Bradley, A.P. 1997, The use of the area under the ROC curve in the evaluation of machine learning algorithms, *Pattern recognition*, 30(7): 1145–1159.
- Breiman, L. 2001, Random Forests, *Machine Learning*, 45(1): 5–32. doi:[10.1023/A:1010933404324](https://doi.org/10.1023/A:1010933404324)
- Carmignani, L., Moncel, M.-H., Fernandes, P. & Wilson, L. 2017, Technological variability during the Early Middle Palaeolithic in Western Europe. Reduction systems and predetermined products at the Bau de l'Aubesier and Payre (South-East France), *PLoS ONE*, 12(6): e0178550. doi:[10.1371/journal.pone.0178550](https://doi.org/10.1371/journal.pone.0178550)
- Casanova i Martí, J., Martínez Moreno, J., Mora Torcal, R. & Torre, I. de la 2009, Stratégies techniques dans le Paléolithique Moyen du sud-est des Pyrénées, *L'Anthropologie*, 113: 313–340. doi:[10.1016/j.anthro.2009.04.004](https://doi.org/10.1016/j.anthro.2009.04.004)
- Casanova, J., Roda Gilabert, X., Martínez-Moreno, J. & Mora, R. 2014, Débitage, façonnage et diversité des systèmes techniques du Moustérien à Tragó (Pré-Pyrénées de Lleida, Catalogne), In: *Transitions, ruptures et continuité en Préhistoire* (J. Jaubert, N. Fourment & P. Depaepe, Eds.), Paris, Société Préhistorique Française: p. 139–154.
- Clarkson, C. 2007, *Lithics in the Land of the Lightning Brothers: The Archaeology of Wardaman Country, Northern Territory*, Canberra, The Australian National University Press.
- Cortes, C. & Vapnik, V. 1995, Support-vector networks, *Machine learning*, 20(3): 273–297.
- Cotterell, B. & Kamminga, J. 1987, The Formation of Flakes, *American Antiquity*, 52(4): 675–708.
- Cover, T. & Hart, P. 1967, Nearest neighbor pattern classification, *IEEE Transactions on Information Theory*, 13(1): 21–27. doi:[10.1109/TIT.1967.1053964](https://doi.org/10.1109/TIT.1967.1053964)
- Cramer, J.S. 2004, The early origins of the logit model, *Studies in History and Philosophy of Science Part C: Studies in History and Philosophy of Biological and Biomedical Sciences*, 35(4): 613–626. doi:[10.1016/j.shpsc.2004.09.003](https://doi.org/10.1016/j.shpsc.2004.09.003)
- Davis, Z.J. & Shea, J.J. 1998, Quantifying lithic curation: An experimental test of Dibble and Pelcin's

- original flake-tool mass predictor, *Journal of Archaeological Science*, 25(7): 603–610.
- Debénath, A. & Dibble, H.L. 1994, *Handbook of Paleolithic Typology*, University of Pennsylvania Press.
- Delagnes, A. 1995, Variability within Uniformity: Three Levels of Variability within the Levallois System, In: *The Definition and Interpretation of Levallois Technology* (H. L. Dibble & O. Bar-Yosef, Eds.), Monographs in World Archaeology., Madison, Wisconsin, Prehistory Press: p. 201–211.
- Delagnes, A., Jaubert, J. & Meignen, L. 2007, Les technocomplexes du paléolithique moyen en Europe occidentale dans leur cadre diachronique et géographique, In: *Les Neandertaliens. Biologie et Cultures* (B. Vandermeersch & B. Maureille, Eds.), Documents préhistoriques., Paris, Editions du Comité des Travaux Historiques et Scientifiques: p. 213–229.
- Delagnes, A. & Meignen, L. 2006, Diversity of Lithic Production Systems During the Middle Paleolithic in France. Are There Any Chronological Trends?, In: *Transitions Before the Transition Evolution and Stability in the Middle Paleolithic and Middle Stone Age* (E. Hovers, S. L. Kuhn & M. Jochim, Eds.), Springer: p. 85–107.
- Dibble, H.L. 1995, Biache Saint-Vaast, Level IIA: A comparison of analytical approaches, In: *The definition and interpretation of Levallois technology* (H. L. Dibble & O. Bar-Yosef, Eds.), Monographs in World Archaeology., Prehistory Press: p. 93–116.
- Dibble, H.L. 1989, The Implications of Stone Tool Types for the Presence of Language During the Lower and Middle Palaeolithic, In: *The Human Revolution: Behavioural and Biological Perspectives on the Origins of Modern Humans* (P. Mellars & C. Stringer, Eds.), Edinburgh, Edinburgh University Press: p. 415–432.
- Dibble, H.L. & Pelcin, A. 1995, The Effect of Hammer Mass and Velocity on Flake Mass, *Journal of Archaeological Science*, 22(3): 429–439. doi:[10.1006/jasc.1995.0042](https://doi.org/10.1006/jasc.1995.0042)
- Driscoll, K. & García-Rojas, M. 2014, Their lips are sealed: Identifying hard stone, soft stone, and antler hammer direct percussion in Palaeolithic prismatic blade production, *Journal of Archaeological Science*, 47: 134–141. doi:[10.1016/j.jas.2014.04.008](https://doi.org/10.1016/j.jas.2014.04.008)
- Eren, M.I., Greenspan, A. & Garth Sampson, C. 2008, Are Upper Paleolithic blade cores more productive than Middle Paleolithic discoidal cores? A replication experiment, *Journal of Human Evolution*, 55: 952–961. doi:[10.1016/j.jhevol.2008.07.009](https://doi.org/10.1016/j.jhevol.2008.07.009)
- Eren, M.I. & Lycett, S.J. 2012, Why Levallois? A Morphometric Comparison of Experimental “Preferential” Levallois Flakes versus Debitage Flakes, *PLoS ONE*, 7(1): e29273. doi:[10.1371/journal.pone.0029273](https://doi.org/10.1371/journal.pone.0029273)
- Faivre, G.-P., Gravina, B., Bourguignon, L., Discamps, E. & Turq, A. 2017, Late Middle Palaeolithic lithic technocomplexes (MIS 5–3) in the northeastern Aquitaine Basin: Advances and challenges, *Quaternary International*, 433: 116–131. doi:[10.1016/j.quaint.2016.02.060](https://doi.org/10.1016/j.quaint.2016.02.060)
- Fisher, R.A. 1936, The use of multiple measurements in taxonomic problems, *Annals of Eugenics*, 7: 179–188.
- Forestier, H. 1993, Le Clactonien: Mise en application d'une nouvelle méthode de débitage s'inscrivant dans la variabilité des systèmes de production lithique du Paléolithique ancien, *Paléo*, 5(1): 53–82. doi:[10.3406/pal.1993.1104](https://doi.org/10.3406/pal.1993.1104)
- Frey, P.W. & Slate, D.J. 1991, Letter recognition using Holland-style adaptive classifiers, *Machine learning*, 6(2): 161–182.
- Friedman, J.H. 2001, Greedy function approximation: A gradient boosting machine, *Annals of statistics*, 29(5): 1189–1232.
- Friedman, J.H. 2002, Stochastic gradient boosting, *Computational Statistics & Data Analysis*, 38(4): 367–378. doi:[10.1016/S0167-9473\(01\)00065-2](https://doi.org/10.1016/S0167-9473(01)00065-2)
- Geneste, J.-M. 1990, Développement des systèmes de production lithique au cours du Paléolithique moyen en Aquitaine septentrionale, In: *Paléolithique Moyen Récent et Paléolithique Supérieur Ancien en Europe* (C. Farizy, Ed.), Mémoires du Musée de Préhistoire d'Ile-de-France., Nemours, APRAIF: p. 203–214.
- González-Molina, I., Jiménez-García, B., Maíllo-Fernández, J.-M., Baquedano, E. & Domínguez-Rodrigo, M. 2020, Distinguishing Discoid and Centripetal Levallois methods through machine learning P. De Smedt, Ed., *PLOS ONE*, 15(12): e0244288. doi:[10.1371/journal.pone.0244288](https://doi.org/10.1371/journal.pone.0244288)
- Greenwell, B., Boehmke, B., Cunningham, J., Developers, G.B.M. & Greenwell, M.B. 2019, Package “gbm,” *R package version*, 2(5).
- Grimaldi, S. & Santaniello, F. 2014, New insights into Final Mousterian lithic production in western Italy, *Quaternary International*, 350: 116–129. doi:[10.1016/j.quaint.2014.03.057](https://doi.org/10.1016/j.quaint.2014.03.057)
- Hérisson, D., Brenet, M., Cliquet, D., Moncel, M.-H., Richter, J., Scott, B., Van Baelen, A., Di Modica, K., De Loecker, D., Ashton, N., Bourguignon, L., Delagnes, A., Faivre, J.-P., Folgado-Lopez, M., Locht, J.-

- L., Pope, M., Raynal, J.-P., Roebroeks, W., Santagata, C., Turq, A. & Van Peer, P. 2016, The emergence of the Middle Palaeolithic in north-western Europe and its southern fringes, *Quaternary International*, 411: 233–283. doi:[10.1016/j.quaint.2016.02.049](https://doi.org/10.1016/j.quaint.2016.02.049)
- Hiscock, P. 2002, Quantifying the Size of Artefact Assemblages, *Journal of Archaeological Science*, 29: 251–258. doi:[10.1006/jasc.2001.0705](https://doi.org/10.1006/jasc.2001.0705)
- Hovers, E. 2009, *The lithic assemblages of Qafzeh Cave*, New York, Oxford University Press.
- James, G., Witten, D., Hastie, T. & Tibshirani, R. 2013, *An Introduction to Statistical Learning with Applications in R*, Second Edition., Springer.
- Jaubert, J. 1993, Le gisement paléolithique moyen de Mauran (Haute-Garonne) : Techno-économie des industries lithiques, *Bulletin de la Société préhistorique française*, 90(5): 328–335. doi:[10.3406/bspf.1993.9642](https://doi.org/10.3406/bspf.1993.9642)
- Karatzoglou, A., Meyer, D. & Hornik, K. 2006, Support Vector Machines in R, *Journal of Statistical Software*, 15: 1–28. doi:[10.18637/jss.v015.i09](https://doi.org/10.18637/jss.v015.i09)
- Karatzoglou, A., Smola, A., Hornik, K. & Zeileis, A. 2004, Kernlab - An S4 Package for Kernel Methods in R, *Journal of Statistical Software*, 11: 1–20. doi:[10.18637/jss.v011.i09](https://doi.org/10.18637/jss.v011.i09)
- Kelly, H. 1954, Contribution à l'étude de la technique de la taille levalloisienne, *Bulletin de la Société Préhistorique Française*, 51(3-4): 149–169. doi:[10.3406/bspf.1954.3077](https://doi.org/10.3406/bspf.1954.3077)
- Kuhn, M. 2008, Building Predictive Models in R using the caret Package, *Journal of Statistical Software*, 28(5). doi:[10.18637/jss.v028.i05](https://doi.org/10.18637/jss.v028.i05)
- Kuhn, S.L. 2013, Roots of the Middle Paleolithic in Eurasia, *Current Anthropology*, 54(S8): S255–S268. doi:[10.1086/673529](https://doi.org/10.1086/673529)
- Lantz, B. 2019, *Machine learning with R: Expert techniques for predictive modeling*, Packt publishing ltd.
- Laplace, G. 1968, Recherches de typologie analytique 1968, *Origini*, II: 7–64.
- Lenoir, M. & Turq, A. 1995, Recurrent Centripetal Debitage (Levallois and Discoidal): Continuity or Discontinuity?, In: *The definition and interpretation of Levallois Technology* (H. L. Dibble & O. Bar-Yosef, Eds.), Monographs in World Archaeology., Madison, Wisconsin, Prehistory Press: p. 249–256.
- Locht, J.-L. 2003, L'industrie lithique du gisement de Beauvais (Oise, France): Objectifs et variabilité du débitage discoïde, In: *Discoid Lithic Technology: Advances and Implications* (M. Peresani, Ed.), BAR International Series., Oxford, Archaeopress: p. 193–209.
- Lombera-Hermida, A. de, Rodríguez-Álvarez, X.P., Mosquera, M., Ollé, A., García-Medrano, P., Pedernana, A., Terradillos-Bernal, M., López-Ortega, E., Bargalló, A., Rodríguez-Hidalgo, A., Saladié, P., Bermúdez de Castro, J.M. & Carbonell, E. 2020, The dawn of the Middle Paleolithic in Atapuerca: The lithic assemblage of TD10.1 from Gran Dolina, *Journal of Human Evolution*, 145: 102812. doi:[10.1016/j.jhevol.2020.102812](https://doi.org/10.1016/j.jhevol.2020.102812)
- Marciani, G., Ronchitelli, A., Arrighi, S., Badino, F., Bortolini, E., Boscato, P., Boschin, F., Crezzini, J., Delpiano, D., Falcucci, A., Figus, C., Lugli, F., Oxilia, G., Romandini, M., Riel-Salvatore, J., Negrino, F., Peresani, M., Spinapolic, E.E., Moroni, A. & Benazzi, S. 2020, Lithic techno-complexes in Italy from 50 to 39 thousand years BP: An overview of lithic technological changes across the Middle-Upper Palaeolithic boundary, *Quaternary International*, 551: 123–149. doi:[10.1016/j.quaint.2019.11.005](https://doi.org/10.1016/j.quaint.2019.11.005)
- Marwick, B. 2008, What attributes are important for the measurement of assemblage reduction intensity? Results from an experimental stone artefact assemblage with relevance to the Hoabinhian of mainland Southeast Asia, *Journal of Archaeological Science*, 35(5): 1189–1200. doi:[10.1016/j.jas.2007.08.007](https://doi.org/10.1016/j.jas.2007.08.007)
- Moncel, M.-H., Ashton, N., Arzarello, M., Fontana, F., Lamotte, A., Scott, B., Muttillo, B., Berruti, G., Nenzioni, G. & Tuffreau, A. 2020, Early Levallois core technology between marine isotope stage 12 and 9 in Western Europe, *Journal of human evolution*, 139: 102735. doi:[10.1016/j.jhevol.2019.102735](https://doi.org/10.1016/j.jhevol.2019.102735)
- Mortillet, G. de 1885, *Le préhistorique. Antiquité de l'homme*, Deuxième Édition., París, Bibliothèque des Sciences Contemporaines., 658 p.
- Mourre, V. 2003, Discoïde ou pas Discoïde? Réflexions sur la pertinence des critères techniques définissant le débitage discoïde, In: *Discoid Lithic Technology. Advances and Implications* (M. Peresani, Ed.), BAR International Series., Oxford, Archaeopress: p. 1–17.
- Muller, A. & Clarkson, C. 2016, A new method for accurately and precisely measuring flake platform area, *Journal of Archaeological Science: Reports*, 8: 178–186. doi:[10.1016/j.jasrep.2016.06.015](https://doi.org/10.1016/j.jasrep.2016.06.015)
- Newcomer, M.H. & Hivernel-Guerre, F. 1974, Nucléus sur éclat: Technologie et utilisation par différentes cultures préhistoriques, *Bulletin de la Société Préhistorique Française*, 71(4): 119–128. doi:[10.3406/bspf.1974.8308](https://doi.org/10.3406/bspf.1974.8308)

- Ohel, M.Y., Bhattacharya, D.K., Bordes, F., Cahen, D., Callow, P., Collins, D., Katz, P.R., Narr, K.J., Newcomer, M.H., Pappu, R.S., Roe, D.A., Singer, R. & Wymer, J.J. 1979, [The Clactonian: An Independent Complex or an Integral Part of the Acheulean? \[And Comments and Reply\]](#), *Current Anthropology*, 20(4): 685–726.
- Pelegrin, J. 2009, Cognition and the emergence of language: A contribution from lithic technology, In: *Cognitive Archaeology and Human Evolution* (S. A. de Beaune, F. L. Coolidge & T. Wynn, Eds.), New York, Cambridge University Press: p. 95–108.
- Peresani, M. 1998, La variabilité du débitage discoïde dans la grotte de Fumane (Italie du Nord)/The variability of discoid production at the grotte de Fumane, *Paléo*, 10: 123–146. doi:[10.3406/pal.1998.1133](https://doi.org/10.3406/pal.1998.1133)
- Perpère, M. 1986, Apport de la typométrie à la définition des éclats Levallois : L'exemple d'Ault, *Bulletin de la Société préhistorique française*, 83(4): 115–118. doi:[10.3406/bfsp.1986.8743](https://doi.org/10.3406/bfsp.1986.8743)
- Perpère, M. 1989, Les frontières du débitage Levallois: Typométrie des éclats, *L'Anthropologie*, 95(4): 837–850.
- Quinlan, J.R. 2014, *C4. 5: Programs for machine learning*, Elsevier.
- Quinlan, J.R. 1996, Improved Use of Continuous Attributes in C4.5, *Journal of Artificial Intelligence Research*, 4: 77–90. doi:[10.1613/jair.279](https://doi.org/10.1613/jair.279)
- Révillon, S. & Tuffreau, A. (Eds.) 1994, *Les industries laminaires au Paléolithique moyen*, Paris, CNRS Editions.
- Ridgeway, G. 2007, [Generalized Boosted Models: A guide to the gbm package](#), *R package vignette*, 2007.
- Ríos-Garaizar, J. 2017, A new chronological and technological synthesis for Late Middle Paleolithic of the Eastern Cantabrian Region, *Quaternary International*, 433: 50–63. doi:[10.1016/j.quaint.2016.02.020](https://doi.org/10.1016/j.quaint.2016.02.020)
- Robin, X., Turck, N., Hainard, A., Tiberti, N., Lisacek, F., Sanchez, J.-C. & Müller, M. 2011, pROC: An open-source package for R and S+ to analyze and compare ROC curves, *BMC bioinformatics*, 12(1): 1–8.
- Rosenberg-Yefet, T., Shemer, M. & Barkai, R. 2022, Lower Paleolithic Winds of Change: Prepared Core Technologies and the Onset of the Levallois Method in the Levantine Late Acheulian, *Frontiers in Earth Science*, 10: 847358. doi:[10.3389/feart.2022.847358](https://doi.org/10.3389/feart.2022.847358)
- Rumelhart, D.E., Hinton, G.E. & Williams, R.J. 1986, Learning representations by back-propagating errors, *Nature*, 323(6088): 533–536.
- Santonja, M., Pérez-González, A., Panera, J., Rubio-Jara, S. & Méndez-Quintas, E. 2016, The coexistence of Acheulean and Ancient Middle Palaeolithic techno-complexes in the Middle Pleistocene of the Iberian Peninsula, *Quaternary International*, 411: 367–377.
- Scott, B. & Ashton, N. 2011, The early middle Palaeolithic: The European context, In: *The ancient human occupation of Britain* (N. Ashton, S. Lewis & C. Stringer, Eds.), Developments in Quaternary Science., Oxford, Elsevier: p. 91–112.
- Shott, M.J. & Seeman, M.F. 2017, Use and multifactorial reconciliation of uniface reduction measures: A pilot study at the Nobles Pond Paleoindian site, *American Antiquity*, 82(4): 723–741. doi:[10.1017/aaq.2017.40](https://doi.org/10.1017/aaq.2017.40)
- Slimak, L. 1998, La variabilité des débitages discoïdes au Paléolithique moyen: Diversité des méthodes et unité d'un concept. L'exemple des gisements de la Baume Néron (Soyons, Ardèche) et du Champ Grand (Saint-Maurice-sur-Loire, Loire), *Préhistoire Anthropologie Méditerranéennes*, 7: 75–88.
- Slimak, L. 2003, Les Débitages discoïdes moustériens: Evaluation d'un concept technologique, In: *Discoid Lithic Technology. Advances and Implications* (M. Peresani, Ed.), BAR International Series., Oxford, Archaeopress: p. 33–65.
- Soressi, M. & Geneste, J.-M. 2011, The History and Efficacy of the Chaîne Opératoire Approach to Lithic Analysis: Studying Techniques to Reveal Past Societies in an Evolutionary Perspective, *PaleoAnthropology*, 2011: 334–350. doi:[10.4207/PA.2011.ART63](https://doi.org/10.4207/PA.2011.ART63)
- Soriano, S. & Villa, P. 2017, Early Levallois and the beginning of the Middle Paleolithic in central Italy M. D. Petraglia, Ed., *PLOS ONE*, 12(10): e0186082. doi:[10.1371/journal.pone.0186082](https://doi.org/10.1371/journal.pone.0186082)
- Spackman, K.A. 1989, Signal detection theory: Valuable tools for evaluating inductive learning, In: *Proceedings of the sixth international workshop on Machine learning*, Elsevier: p. 160–163.
- Team, R.C. 2019, [R: A language and environment for statistical computing](#).
- Team, Rs. 2019, [RStudio: Integrated Development for R](#).
- Terradas, X. 2003, Discoid flaking method: Conception and technological variability, In: *Discoid Lithic Technology. Advances and Implications* (M. Peresani, Ed.), BAR International Series., Oxford, Archaeopress:

p. 19–32.

- Thiébaut, C. 2013, Discoid debitage stricto sensu: A method adapted to highly mobile Middle Paleolithic groups?, *P@lethnology*, Varia.
- Tixier, J. & Turq, A. 1999, Kombewa et alii, *Paléo*, 11: 135–143. doi:[10.3406/pal.1999.1174](https://doi.org/10.3406/pal.1999.1174)
- Torre, I. de la, Mora, R., Domínguez-Rodrigo, M., Luque, L. de & Alcalá, L. 2003, The Oldowan industry of Peninj and its bearing on the reconstruction of the technological skills of Lower Pleistocene hominids, *Journal of Human Evolution*, 44(2): 203–224. doi:[10.1016/S0047-2484\(02\)00206-3](https://doi.org/10.1016/S0047-2484(02)00206-3)
- Venables, W.N. & Ripley, B.D. 2002, *Modern applied statistics with S*, Fourth Edition., New York, Springer.
- Walker, S.H. & Duncan, D.B. 1967, Estimation of the Probability of an Event as a Function of Several Independent Variables, *Biometrika*, 54(1/2): 167–179. doi:[10.2307/2333860](https://doi.org/10.2307/2333860)
- White, M. & Ashton, N. 2003, Lower Palaeolithic Core Technology and the Origins of the Levallois Method in North-Western Europe, *Current Anthropology*, 44(4): 598–609.
- Wickham, H., Averick, M., Bryan, J., Chang, W., McGowan, L., François, R., Grolemund, G., Hayes, A., Henry, L., Hester, J., Kuhn, M., Pedersen, T., Miller, E., Bache, S., Müller, K., Ooms, J., Robinson, D., Seidel, D., Spinu, V., Takahashi, K., Vaughan, D., Wilke, C., Woo, K. & Yutani, H. 2019, Welcome to the Tidyverse, *Journal of Open Source Software*, 4(43): 1686. doi:[10.21105/joss.01686](https://doi.org/10.21105/joss.01686)
- Wright, M.N. & Ziegler, A. 2017, Ranger: A Fast Implementation of Random Forests for High Dimensional Data in C++ and R, *Journal of Statistical Software*, 77: 1–17. doi:[10.18637/jss.v077.i01](https://doi.org/10.18637/jss.v077.i01)